Sediment routing and basin evolution in Proterozoic to Mesozoic east Gondwana: a case study from southern Australia

M. Barham[1], S. Reynolds[1], C.L. Kirkland[1,2], M.J. O'Leary[1,3], N.J. Evans[1,4], H.J. Allen[5], P.W. Haines[5], R.M. Hocking[5], and B.J. McDonald[1,4]

[1]*The Institute for Geoscience Research (TIGeR), School of Earth and Planetary Sciences, Curtin University, GPO Box U1987, Perth, WA 6845, Australia*

[2]*Centre for Exploration and Targeting (CET), Curtin University, GPO Box U1987, Perth, WA 6845, Australia*

[3]*School of Molecular and Life Sciences, Curtin University, GPO Box U1987, Perth, WA 6845, Australia*

[4]*John de Laeter Center, Curtin University, GPO Box U1987, Perth, WA 6845, Australia*

[5]*Geological Survey of Western Australia, 100 Plain St., East Perth, WA 6004, Australia*

Key words: Bight Basin, Madura Shelf, geochronology, Hf, provenance, detrital zircon

ABSTRACT

Sedimentary rocks along the southern margin of Australia host an important record of the break-up history of east Gondwana, as well as fragments of a deeper geological history, which collectively help inform the geological evolution of a vast and largely underexplored region. New drilling through Cenozoic cover has allowed examination of the Cretaceous rift-related Madura Shelf sequence (Bight Basin), and identification of two new stratigraphic units beneath the shelf; the possibly Proterozoic Shanes Dam Conglomerate and the interpreted Palaeozoic southern Officer Basin unit, the Decoration Sandstone. Recognition of these new units indicates an earlier basinal history than previously known.

Lithostratigraphy of the new drillcore has been integrated with that published from onshore and offshore cores to present isopach maps of sedimentary cover on the Madura Shelf. New palynological data demonstrate progression from more localized freshwater-brackish fluvio-lacustrine clastics in the early Cretaceous (*Foraminisporis wonthaggiensis* – Valanginian to Barremian) to widespread topography-blanketing, fully marine, glauconitic mudrocks in the mid Cretaceous (*Endoceratium ludbrookiae* – Albian).

Geochronology and Hf-isotope geochemistry show detrital zircon populations from the Madura Shelf are comparable to those from the southern Officer Basin, as well as Cenozoic shoreline and palaeovalley sediments in the region. The detrital zircon population from the Shanes Dam Conglomerate is defined by a unimodal ~1400 Ma peak, which correlates with directly underlying crystalline basement of the Madura Province. Peak ages of ~1150 Ma and ~1650 Ma dominate the age spectra of all other samples, indicating a stable sediment reservoir through much of the Phanerozoic, with sediments largely sourced from the Albany-Fraser and Musgrave Orogens (directly and via multiple recycling events). The Madura Shelf data differ from published data for the Upper Cretaceous Ceduna Delta to the east, indicating significant differences in sediment provenance and routing between the Ceduna Sub-basin and central Bight Basin.

1 INTRODUCTION

Sedimentary rocks provide an important record of their eroded source region(s) and the opportunity to chart long-term changes in Earth-surface conditions. Analysis (compositional, geochronological and geochemical) of detrital minerals allows greater resolution of the overall tectonic framework and geological history of a region than can be discerned from primary basement outcrops (and subcrops) alone (Carrapa, 2010; Cawood et al., 2012; Dhuime et al., 2011; Dickinson and Suczek, 1979; Iizuka et al., 2013; Kemp et al., 2006; Maidment et al., 2007; McCann and Saintot, 2003; O'Sullivan et al., 2016; Tucker et al., 2016). With an increasingly comprehensive geological understanding of regional crystalline basement blocks, geochronology and geochemistry of detrital minerals are becoming established as powerful techniques to elucidate palaeogeographic and stratigraphic relationships, as well as uplift, erosion and sediment routing histories (Cawood and Nemchin, 2000; Fielding et al., 2017; Kirkland et al., 2007; Lancaster et al., 2017; Mark et al., 2016; Tyrrell et al., 2007; Xu et al., 2016).

The extensive passive margin defining the southern limit of the Australian continent was formed during the ultimate Mesozoic break-up phase of Gondwana as Australia rifted away from Antarctica (Brown et al., 2003). This separation ended over a billion years of shared history between the Australian and Antarctic continents (Cawood and Korsch, 2008; Huston et al., 2012; Johnson, 2013) and reshaped their surface environments. Prior to this, the Proterozoic assembly of the West Australian Craton (WAC) and North Australian Craton with the South Australian Craton (SAC) and its Antarctic extension (Mawson Craton; Fitzsimons, 2003; Goodge and Fanning, 2016; Huston et al., 2012; Johnson, 2013; Payne et al., 2009) had resulted in well-defined orogenic belts with enhanced mineral endowment facilitated by crustal-scale tectonic structures, juvenile mantle input, crustal reworking, disturbed thermal gradients and fluid migration (Groves and Bierlein, 2007; Huston et al., 2012; Jaques et al., 2002; Leahy et al., 2005; Wyborn et al., 1994). Unfortunately, little evidence of post-assembly Neoproterozoic to Mesozoic events is preserved at the surface on the southern margin of Australia, while equivalent geology on Antarctica is largely ice-covered and inaccessible. Between the WAC and the SAC, a blanket of Eocene and Miocene carbonates and associated clastics (Eucla Basin) form the present-day Nullarbor Plain, which obscures almost a quarter of a million square kilometres of underlying sedimentary and basement rocks (Fig. 1). Consequently, the Proterozoic to Cenozoic geological history of central southern Australia is very poorly understood.

With growing awareness of the importance of suture zones in regions of enhanced mineral fertility (e.g. Groves and Santosh, 2015; Jaques et al., 2002; Kirkland et al., 2015b), interest in the potential continuation of mineralization associated with the edge of the Yilgarn Craton margin beneath central southern Australia has increased (Spaggiari and Smithies, 2015). Furthermore, offshore Mesozoic sedimentary basins along the southern Australian margin represent sites of frontier hydrocarbon exploration, and world-class heavy mineral sand deposits are mined along Cenozoic palaeoshorelines (Hou et al., 2011; Reid et al., 2013). Despite this collective recognition of the significant economic potential of the region, and a capacity to further understanding of Australia-Antarctica separation, pre-Cenozoic sediments of southern Australian basins between the WAC and SAC remain relatively understudied as a result of remoteness and lack of outcrop. However, new drillcore produced through the Western Australian governments' Exploration Incentive Scheme has uncovered new information, described here, about sedimentary packages sandwiched between the obscured Mesoproterozoic basement and overlying Cenozoic carbonates.

The work reported herein integrates new and existing observations on sedimentology, stratigraphic architecture, detrital mineral provenance, and palynology, to facilitate a robust analysis of sedimentation in central southern Australia from the Proterozoic to mid Cretaceous. Zircon Hf-isotopic geochemistry combined with U/Pb geochronology provides a more refined mechanism to characterize sediment source areas; especially in regions that may have shared similar timings of igneous events but with different magmatic sources. Reconstruction of evolving palaeoenvironmental conditions on Australia's southern margin, and comparison of sediment character with adjacent depocenters provides insight into the timing of key basinal and regional events, such as mechanical and thermal subsidence, sediment sourcing, and depocenter connectivity and help improve understanding of the geodynamic history of the region.

2 GEOLOGICAL BACKGROUND

The Nullarbor Plain along central southern Australia's margin is underlain in turn by the Cenozoic Eucla Basin, the Cretaceous Madura Shelf of the Bight Basin, the Neoproterozoic-Palaeozoic Officer Basin, and Proterozoic basement (Fig. 1). The region is flanked by the crystalline Archean Yilgarn Craton and its southeastern Palaeo- to Meso-Proterozoic-modified Albany-Fraser Orogen (AFO) margin to the west, the Mesoproterozoic Musgrave Province to the north and the Archean Gawler Craton to the east (Fig. 1). Published mineral geochronology and geochemistry datasets from these crystalline source regions provide age and isotopic characteristics with which to assess the provenance of later sediments that are preserved on or adjacent to these basement rocks (Belousova et al., 2009; Kirkland et al., 2013a; 2015a; 2017; Kositcin, 2010a; Spaggiari et al., 2015).

In the late Palaeoproterozoic-Mesoproterozoic, subduction and island-arc collisions preceding the eventual Mesoproterozoic amalgamation of cratonic Australia are recorded in the Musgrave Province of central Australia, Albany-Fraser Orogen of southwestern Australia and Wilkes Orogen in Antarctica (Cawood and Korsch, 2008; Johnson, 2013; Kirkland et al., 2015a). Previously, very little was known about the basement architecture beneath the Madura Shelf but recent deep seismic and drillcores have revealed the presence of crystalline rocks that demonstrate the existence of a sutured Proterozoic ocean between the Yilgarn and Gawler Cratons (Kirkland et al., 2017; Korsch et al., 2014; Spaggiari and Smithies, 2015). This inter-cratonic region forms the basement to the majority of the area studied here (Fig. 1), and is defined by the Madura and Coompana Provinces, which exhibit isotopic and geochemical signatures indicating an oceanic affinity (Kirkland et al., 2017). Plutonic remnants of an oceanic magmatic arc, the Loongana Arc, have also been identified in the Madura Province (Haig Cave Supersuite; Spaggiari et al., 2014). Significant magmatism and crustal suturing had ceased by the late Mesoproterozoic (late Stenian) assembly of Rodinia, with sedimentary processes dominating the geological record for the next billion years (Cawood and Korsch, 2008).

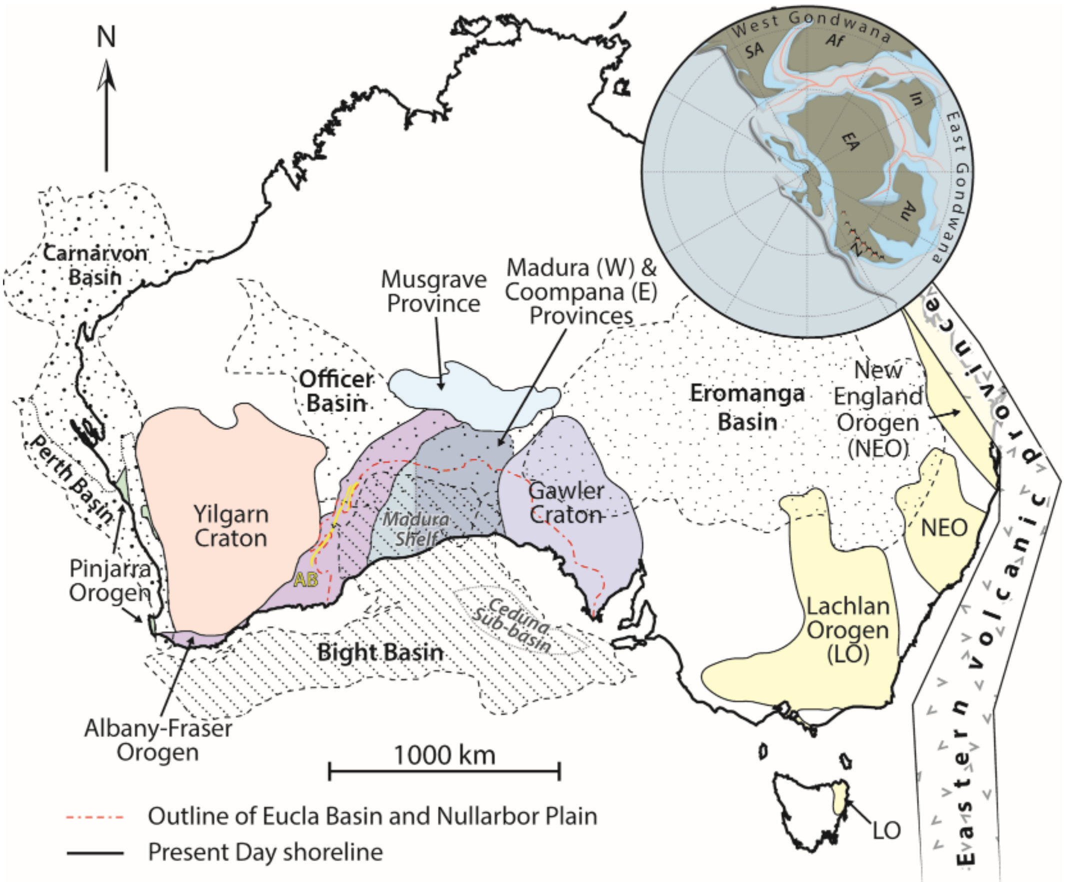

Fig. 1 Map of the major crustal elements of parts of the southern and eastern margins of Australia relevant to this work with overlying selected sedimentary basins. Palaeoshorelines define the limits of the Eucla Basin. "Eastern volcanic province" corresponds to the siliceous large igneous province of Bryan et al. (2012). AB on main map indicates the outcrop of the Arid Basin of the Albany-Fraser Orogen. Only present-day outcrops of the Pinjarra Orogen

are shown on the west coast of Australia, with the rest hidden under the Perth and Carnarvon Basins (not shown). Inset globe shows a general early Cretaceous palaeogeographic reconstruction centred on the south pole; Af – Africa, Au – Australia, EA – East Antarctica, In – India, SA – South America, Z – Zealandia (modified from Blakey, 2008).

A vast (approximately half a million square kilometres) region of sedimentary rocks (primarily the Neoproterozoic-Palaeozoic Officer Basin, Mesozoic Madura Shelf and Cenozoic Eucla Basin) is preserved in the area bound by the AFO, Musgrave Province and Gawler Craton. Offshore, an even greater area of sedimentary rocks is preserved in the remainder of the Mesozoic Bight Basin, extending for over 2000 km along the southern margin of Australia and encompassing several sub-basins, intervening highs (including the Madura Shelf) and the largest delta preserved in Australia today (Upper Cretaceous Ceduna Delta; Fig. 1). Separation of Australia and Antarctica was initiated by Mesozoic crustal thinning, and characterized by brittle upper crustal extension that progressed eastwards from the Late Jurassic (Bradshaw et al., 2003; Totterdell et al., 2000; Willcox and Stagg, 1990). Initially, sedimentation was largely restricted to a series of half-grabens now offshore, but later became more widespread, in response to regional thermal subsidence and global eustatic high sea-levels (Cloetingh and Haq, 2015; Conrad, 2013; Totterdell and Krassay, 2003). This Cretaceous transgression facilitated sedimentation that defines the preserved Madura Shelf, which overlies Officer Basin sediments in the north and sits directly on the AFO and Madura Province in the west and the Coompana Province in the east. Accelerated rifting in the Eocene resulted in an open seaway between Australia and Antarctica and the establishment of an extensive carbonate province across several thousand kilometres of Australia's southern margin (Eucla Basin; Clarke et al., 2003).

The stratigraphy of the Madura Shelf (Fig. 2) and overlying Cenozoic Eucla Basin was largely established by Lowry (1970) who recognized an irregular distribution of coarse clastics (Loongana Formation) that are conformably succeeded by silts and fine sands of the Madura Formation. Deposition was terminated by exposure in the late Cretaceous, and a hiatus of 25-60 Myr separates the Mesozoic sequence from the overlying limestone-dominated (Eocene to Miocene) Hampton Sandstone and Eucla Group carbonate succession comprising the Wilsons Bluff, Abrakurrie and Nullarbor Limestones (Reynolds, 2016). Each of the carbonate units are separated by disconformities representing successive marine transgressions and regressions (Hou et al., 2008).

3 MATERIALS AND METHODS

3.1 Boreholes

Samples and new lithostratigraphical data were derived from drillcore housed at the Geological Survey of Western Australia (GSWA) Perth Core Library at Carlisle, Perth, and initially presented as an undergraduate honours thesis (Reynolds, 2016). Zircon geochronology/geochemistry and dinocyst palynology from a single sample from the upper Madura Formation (199453) were reported in Barham et al. (2016) but are included here for a more complete basinal synthesis. In total, three new GSWA cores (FOR004, FOR010, FOR011) drilled during the 2013/2014 Eucla basement drilling program were logged, in addition to four cores that recently became public (HDDH001, HDDH002, SDDH001, SDDH002; Supplementary Fig. 1). All new stratigraphic data were integrated with published material from the Madura Shelf across Western Australia and South Australia states (Fig. 3; Supplementary Table 1). Metre values quoted in this work correspond to depth in the respective cores, while data normalized to elevation above sea-level (calculated from collar elevations, drilling angles and known deviations) are suffixed with AHD (Australian Height Datum).

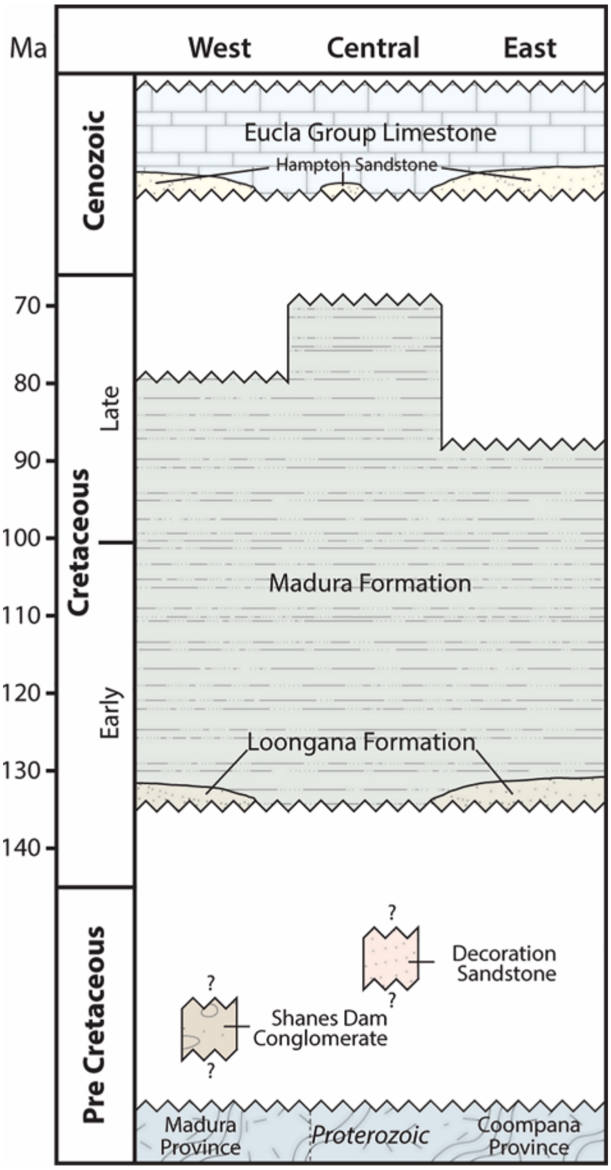

Fig. 2 Simplified stratigraphy of the study region in southern Australia.

3.2 Palynostratigraphy

Six organic-rich mud-grade lithological samples were submitted for palynological processing at MGPalaeo (Fig. 3). Palynostratigraphical designations were based on standard 100 specimen counts, as well as identification of other key palynomorphs, on prepared slides.

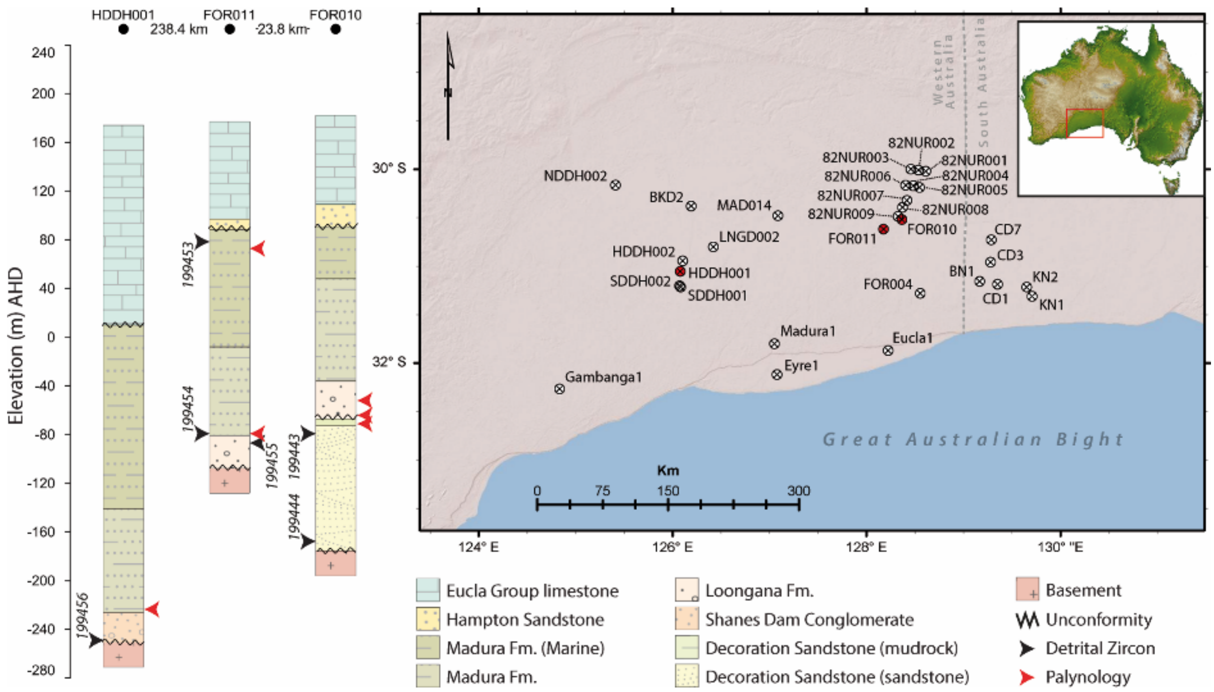

Fig. 3 Location map of studied boreholes/wells and stratigraphy of sampled sequences. Wells highlighted in red correspond to those sampled for palynology and detrital zircon geochronology in this study.

3.3 Detrital mineral preparation

Eight ~1kg, dominantly arenaceous core samples were submitted for mineral processing with a focus on extraction of zircon. Cemented samples were disaggregated using SELFRAG and heavy mineral phases concentrated via standard panning, polytungstate-based heavy-liquid flotation and Frantz magnetic separation. Representative zircon grains from heavy mineral concentrates were mounted in rows on double sided tape attached to glass plates along with zircon standards BR266, TEMORA II, CZ3, and OG1 within 10 mm diameter circular areas. Epoxycure resin was used to produce 25 mm diameter mounts, which were polished (to a 1 µm finish) back to approximate half-grain thickness to expose internal grain structure. Mounted grains were imaged using standard light microscopy, back-scattered electron microscopy and cathodoluminescence electron microscopy using a $MIRA_3$ VP-FESEM at the Microscopy and Microanalysis Facility, John de Laeter Centre, Curtin University. Inclusions, metamict zones or grains with polyphase growth histories identified during microscopic examination were subsequently avoided during grain geochronological and geochemical analyses. Oscillatory zoned regions of grains were targeted to obtain crystallization ages.

3.4 U/Pb zircon geochronology

Isotopic compositions of zircon mineral fractions were analysed using laser ablation inductively coupled plasma mass spectrometry (LA-ICP-MS) at the GeoHistory Facility, John de Laeter Centre, Curtin University. Targeted portions of individual zircon grains were ablated using a Resonetics M-50 193nm ArF excimer laser with isotopic intensities measured using an Agilent 7700s quadrupole ICP-MS, with high purity Ar as the carrier gas. Elements ^{28}Si, ^{29}Si, ^{204}Pb, ^{206}Pb, ^{207}Pb, ^{208}Pb, ^{232}Th, and ^{238}U were monitored for 0.03 seconds each. Following 10 s of background analysis, samples were spot ablated for 30 s using a 33 μm beam, laser energy of 2.5 J/cm^2 and a 7 Hz repetition rate. The sample cell was flushed with ultrahigh purity He (0.68 L min^{-1}) and N_2 (2.8 mL min^{-1}). Natural lead concentration was monitored throughout the analysis, however, no ^{204}Pb was resolved above the level of detection and no natural lead correction has been applied. Plesovice (337.13 ± 0.37 Ma; Sláma et al., 2008) was utilised as the primary age standard in this study, with 91500 (1062.4 ± 0.4 Ma; Wiedenbeck et al., 1995) and GJ-1 (608.5 ± 1.5 Ma; Jackson et al., 2004) used as secondary age standards. $^{206}Pb/^{238}U$ ages calculated for all secondary zircon standards were treated as unknowns and found to be within 3% of the accepted value. Data were reduced in Iolite (U/Pb Geochron4; Paton et al., 2011) and in-house excel macros. All data are reported as $^{207}Pb/^{206}Pb$ ages where grains are >1500 Ma and $^{206}Pb/^{238}U$ for analyses < 1500 Ma (Spencer et al., 2016). Detrital zircon data are considered concordant within 10% of age agreement between the $^{207}Pb/^{206}Pb$ and $^{206}Pb/^{238}U$ systems. Detrital zircon population ages were assessed using the software *isoplot 4.15* (Ludwig, 2012), with Excel macros available from the Arizona Laserchron Centre website (http://www.geo.arizona.edu/alc) used to produce detrital zircon age normalised probability density plots (PDP). Peak ages were assessed with the *AGE PICK* analytical tool (Gehrels et al., 2008), while kernel density plots of detrital zircon age populations, and comparisons of detrital zircon age populations between samples (multidimensional scaling - MDS) were performed in the R statistical "provenance" analysis package (Vermeesch et al., 2016). MDS is based on dissimilarity measures derived from the Kolmogorov–Smirnov test, which investigates the null hypothesis that two distributions (in this case of detrital zircon population ages) are the same, and is derived from the vertical distance between sample cumulative distribution curves of grain ages.

3.5 Lu/Hf zircon geochemistry

Hafnium isotope analyses were subsequently undertaken on the same zircon grains subjected to U/Pb geochronology, using a New Wave/Merchantek LUV213 laser-ablation microprobe, attached to a Nu Plasma multi-collector inductively coupled plasma mass spectrometer, housed at GEMOC, Macquarie University, Sydney. Analytical procedures followed those described in Griffin et al. (2000) and outlined below. Analyses involved a c. 40 µm diameter laser beam with ablation pits 40–60 µm deep. The ablated sample material was transported from the laser cell to the ICP–MS torch in a helium gas flow. Interference of ^{176}Lu on ^{176}Hf was corrected by measurement of the interference-free ^{175}Lu and using an invariant $^{176}Lu/^{175}Lu$ correction factor. Isobaric interference of ^{176}Yb on ^{176}Hf was corrected by measurement of the interference-free ^{172}Yb isotope and using the $^{176}Yb/^{172}Yb$ ratio to calculate the intensity of interference free ^{176}Yb. The appropriate value of $^{176}Yb/^{172}Yb$ was determined by successive doping of the JMC475 Hf standard with various amounts of Yb.

Zircon grains from the Mud Tank carbonatite locality were analysed, together with the samples, as a measure of the accuracy of the results. Most of the data and the mean $^{176}Hf/^{177}Hf$ value (0.282533 ± 32, n = 81) are within two standard deviations of the recommended value (0.282522 ± 42, 2σ; Griffin et al., 2007). Temora-2 zircon was analysed as an independent check on the accuracy of the Yb correction. Temora zircon has an average $^{176}Yb/^{177}Hf$ ratio of 0.04, which is similar to the median $^{176}Yb/^{177}Hf$ ratio of zircon in this study (0.04, n = 77). The average $^{176}Hf/^{177}Hf$ ratio for the analysed Temora-2 was (0.282693 ± 34, n= 56) consistent with the published value for the Temora-2 standard (0.282687 ± 24, LA-ICP-MS; Hawkesworth and Kemp, 2006). Calculation of εHf values employs the decay constant of Scherer et al. (2001) and the chondritic uniform reservoir (CHUR) values of Blichert-Toft and Albarède (1997). We report model ages (T_{DM}^2) calculated as two-stage evolution lines assuming that the parental magma was produced from an average continental crust ($^{176}Lu/^{177}Hf$ = 0.015) that originally was derived from a depleted-mantle source with $(^{176}Hf/^{177}Hf)_i$ = 0.279718 at 4.56 Ga and $^{176}Lu/^{177}Hf$ = 0.0384 (Griffin et al., 2004).

4 RESULTS

4.1 Regional stratigraphy

All boreholes encountered crystalline basement, typically in the form of granitic gneiss. In some cores in the west (e.g. HDDH001), up to 20 m of quartz-rich, mottled saprolitic regolith immediately overlies fresh crystalline rock. Two new units (Shanes Dam Conglomerate and Decoration Sandstone; Reynolds, 2016) have been established as a result of this work, in distinct sedimentary packages disconformable beneath classic Mesozoic rift-related Madura Shelf sediments (Fig. 2).

4.1.1 Shanes Dam Conglomerate

The Shanes Dam Conglomerate is present in four cores; HDDH001, HDDH002, SDDH001 and SDDH002 in the west of the study area, and ranges from <1–25 m in thickness (Fig. 3-4). In all wells, the unit is nonconformable on crystalline basement of the Madura Province and is disconformably overlain by the Madura Formation. The disconformity with the Madura Formation is most distinct in SDDH002 at 413 m depth, where highly ferruginised conglomerate is succeeded by unaltered Madura Fm. (Supplementary Fig. 2). The conglomerate is oligo- to poly-mict, with typically well rounded sandstone, soft green and white claystone, vein quartz, mafic and gneissic/granitic clasts identifiable. Clasts typically range from 1 to 20 mm in size, with a maximum of 60 mm. The unit is commonly highly magnetic, clast-supported and well-indurated, with carbonate cementation variable throughout.

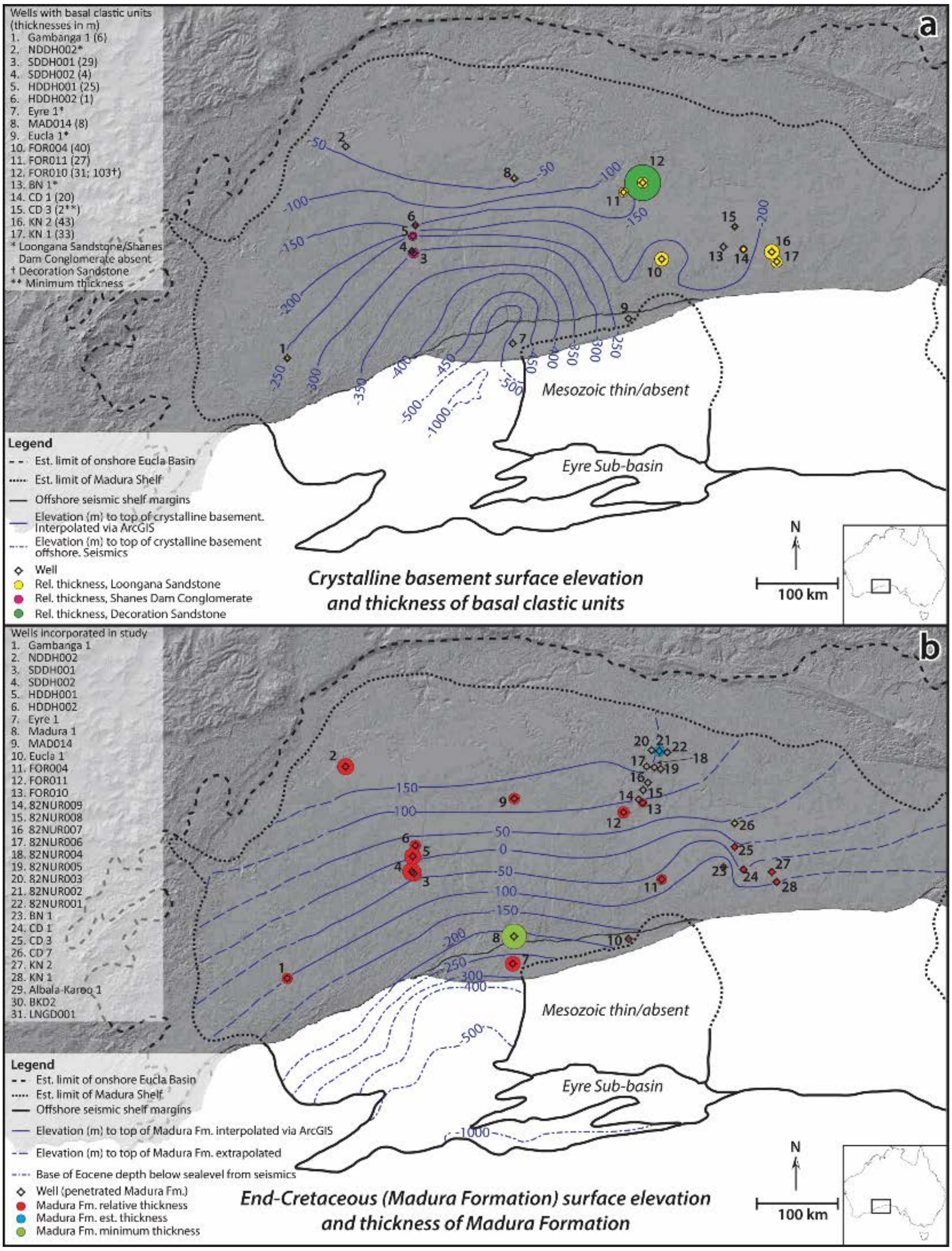

Fig. 4 Sediment thickness and stratigraphic horizon elevation maps of the Madura Shelf. a – basal clastic units (Shanes Dam Conglomerate, Decoration Sandstone and Loongana Sandstone); b – Madura Formation. Offshore depth to horizons inferred from seismic data (JNOC, 1992).

4.1.2 Decoration Sandstone

The Decoration Sandstone was encountered in a single well (FOR010) underlying the central Madura Shelf, where it is 109 m thick (249.3-357.62 m depth, Fig. 3-4). FOR011, less than 24 km from FOR010, intersected no equivalent stratigraphy. The Decoration Sandstone nonconformably overlies crystalline basement of the Coompana Province and is disconformably overlain by carbonaceous mud-grade sediments attributed to the Loongana Formation, with eroded cm-scale clasts incorporated into the overlying unit.

The Decoration Sandstone is predominantly a red-bed sandstone, with the unit broadly divisible into three sections based on facies, the degree of oxidation and hyperspectral data (Supplementary Fig. 1):

- The uppermost six metres (249.3-255.05 m) consists of faintly laminated mottled green and red mudrock. An interval of 20 cm appears to be an exposure surface. The contact with underlying sandstone appears sharp. However, given the similarity of the green silts in the mudrock sequence and finer intervals of the underlying sand-grade dominated succession, and absence of definitive evidence of a significant temporal break, the mudrock is included in the Decoration Sandstone for this work.
- A pale, reduced section from 255.05 m to 295.4 m comprises a fining-upward succession of white sandstone and pale green mudstone interbeds comparable to the overlying mudrock unit. The lower contact is gradational.
- A basal hematite rich, oxidised zone from 295.4 m to 358 m consists of a basal pebbly conglomerate with several pebbly horizons and alternating >1 m thick beds of massive, fining-upwards, planar- and irregular-stratified sands. The irregular-stratified sands have a distinctive wavy/irregular fabric that is interpreted as a product of both intense horizontal bioturbation and fluid disturbance. Conclusive dish and other fluid structures

and vertical burrows up to 1.5 cm wide and 6 cm deep, are also apparent (Supplementary Fig. 2).

Overall the sand is quartz dominated with minor hematite and lithic grains. Grains range from <0.1 to 0.5 mm in size, average ~0.3 mm and are moderately to poorly sorted with the coarser grains being highly spherical and well rounded. The upper sandstone section is lithologically and texturally similar to the basal section but lacks pebble conglomerate and hematite stained levels. Instead, pyrite nodules are common. The upper section also exhibits soft-sediment deformation and fine green muddy laminations with similar patterns to the wavy bedding observed lower in the formation.

4.1.3 Madura Shelf sediments

The Madura Shelf sequence is represented by two formations, with a conformable, commonly gradational contact. The basal Loongana Formation is intersected in nine of the wells studied (Supplementary Table 1) and is thickest (20-40 m) and most commonly developed in the southeast (Fig. 4). It nonconformably overlies crystalline basement in all wells except (i) FOR010 where it disconformably overlies the Decoration Sandstone, and (ii) KN 1 where it overlies Permian sandstone in South Australia. The Loongana Formation typically comprises very poorly consolidated quartz dominated, feldspathic sand with minor mica. As a result of its lack of cementation, little information is retained about original depositional sedimentary structures. The sediment is grain-supported and particles are typically angular, low sphericity, and poorly sorted. Grain sizes are estimated to average 0.5 mm to 1 mm but grains up to 5 mm in size are common.

The Madura Formation is the thickest and most laterally extensive unit of the onshore Bight Basin and is intersected in all the wells studied (Fig. 4; Supplementary Table 1). The formation reaches a thickness of at least 355 m in Madura 1, where it is intersected between -180 m and -535 m (AHD) without encountering the base of the unit. In general, the unit thins towards the basin margins, but remains relatively thick in central areas. The Madura Formation is anomalously thin in wells Eucla 1 and BN 1, where only 30 m and 21 m of the unit are preserved, respectively (Fig. 4).

Where penetrated, the Madura Formation variously conformably overlies the Loongana Formation; disconformably overlies Shanes Dam Conglomerate; or nonconformably overlies crystalline basement (eastern Nornalup Zone, Albany-Fraser Orogen - NDDH002 and Coompana Province - Eucla 1). The Madura Formation is disconformably overlain across the region by Cenozoic units, and typically the Hampton Sandstone, which transitions to carbonates of the Eucla Group.

Lithologically the base of the Madura Formation typically consists of a finer sandy, micaceous and carbonaceous (occasionally charcoal-rich) interval. The formation fines upwards and is dominated by initially barren light grey siltstone and subordinate beds of fine sandstone. Characteristically the upper levels of the formation become increasingly glauconitic, bioturbated and fossiliferous (Supplementary Fig. 2). Most bioclasts are fragmented, though more complete brachiopods, as well as nektic belemnites and coiled cephalopods of unknown designation were identified. In many of the wells, distinct 10-20 cm thick carbonate-cemented horizons are developed within thicker sections of monotonous siltstone.

4.2 Palynology

Five samples (Loongana and Madura Formations; Fig. 3) yielded palynomorph assemblages sufficient to designate a biostratigraphic zone/age to the sample according to the Cretaceous zones of the Great Australian Bight (Partridge, 2006). A sample from finer facies at the top of the Decoration Sandstone (252.9-252.95 m) in FOR010 proved essentially barren of in-situ palynomorphs, with uncommon dinocysts attributed to mud contamination. Complete counts of identified taxa are presented in Supplementary Table 2.

Samples from the Loongana Formation in the FOR010 borehole (235.9-235.92 m and 244.3-244.5 m) contained a distinctive and rich palynomorph assemblage, dominated primarily by the spore/pollen *Microcachryidites antarticus* and *Corollina torosa* and with important occurrences of *Dictyosporites speciousus* and *Cicatricosisporites hughesii* attributed to the *Foraminisporis wonthaggiensis* spore-pollen zone (~ *Senoniasphaera tabulate* Dinocyst Zone) indicating an Early Cretaceous age. Significant numbers of low salinity/freshwater algae taxa (*Microfasta*, *Sigmopollis*, *Horologinella*, *Botryococcus*, etc.) were also recovered.

Samples from basal portions of the Madura Formation in both the HDDH001 (397.6-397.7 m) and FOR011 (256.8-257 m) yielded extremely similar assemblages despite a separation of ~275 km. Samples comprise a rich and distinctive assemblage dominated by the spore/pollen *Dictyophyllidites harrisii*, *Corollina torosa* and a diverse suite of *Retitriletes* spp. and including the stratigraphically significant taxa *Dictyosporites speciousus* and *Retitriletes watharooensis*. No specimens of *Cicatricosisporites* or other distinctive marker taxa were recovered and a *Foraminisporis wonthaggiensis* Zone designation is suggested. Several low-salinity algae taxa were recovered in high numbers, including, but not limited to, *Microfasta*, *Sigmopollis*, *Horologinella*, *Botryococcus*.

The uppermost Madura Formation sampled in FOR011 (104.25-104.4 m) contained an extremely distinctive and rich dinocyst-dominated palynomorph assemblage (Barham et al., 2016). Key dinocyst taxa identified include *Pseudoceratium exuisitum*, *P. turneri*, *Cyclonephelium compactum*, *Litosphaeridium arundum*, *Diconodinium cristatum*, *D.*

psilatum and *D. tuberculatum*. These, in conjunction with the spore pollen taxa *Pilosisporites notensis,* common *Dictyophyllidites harrisii*, *Falcisporites grandis* and *Gleichenidites* spp. suggest an Albian (*Endoceratium ludbrookiae* Zone) age and marine conditions.

4.3 Geochronology

A total of 1023 zircon grains were analysed from six samples (770 from five previously unreported samples and 253 analyses from a previously reported sample; Barham et al., 2016), with 729 of these within 10% of the concordia curve (Fig. 3, 5-6, Supplementary Table 3-4). All samples from the Decoration Sandstone, Loongana Formation and Madura Formation exhibit major concordant age peaks at c. 1150 and 1650 Ma, while zircon grains in Shanes Dam Conglomerate are represented by a single, well-defined concordant c. 1412 Ma peak (Fig. 5-6). Sample 199453, from the upper Madura Formation (FOR011) also records a significant age peak at c. 106 Ma (Barham et al., 2016).

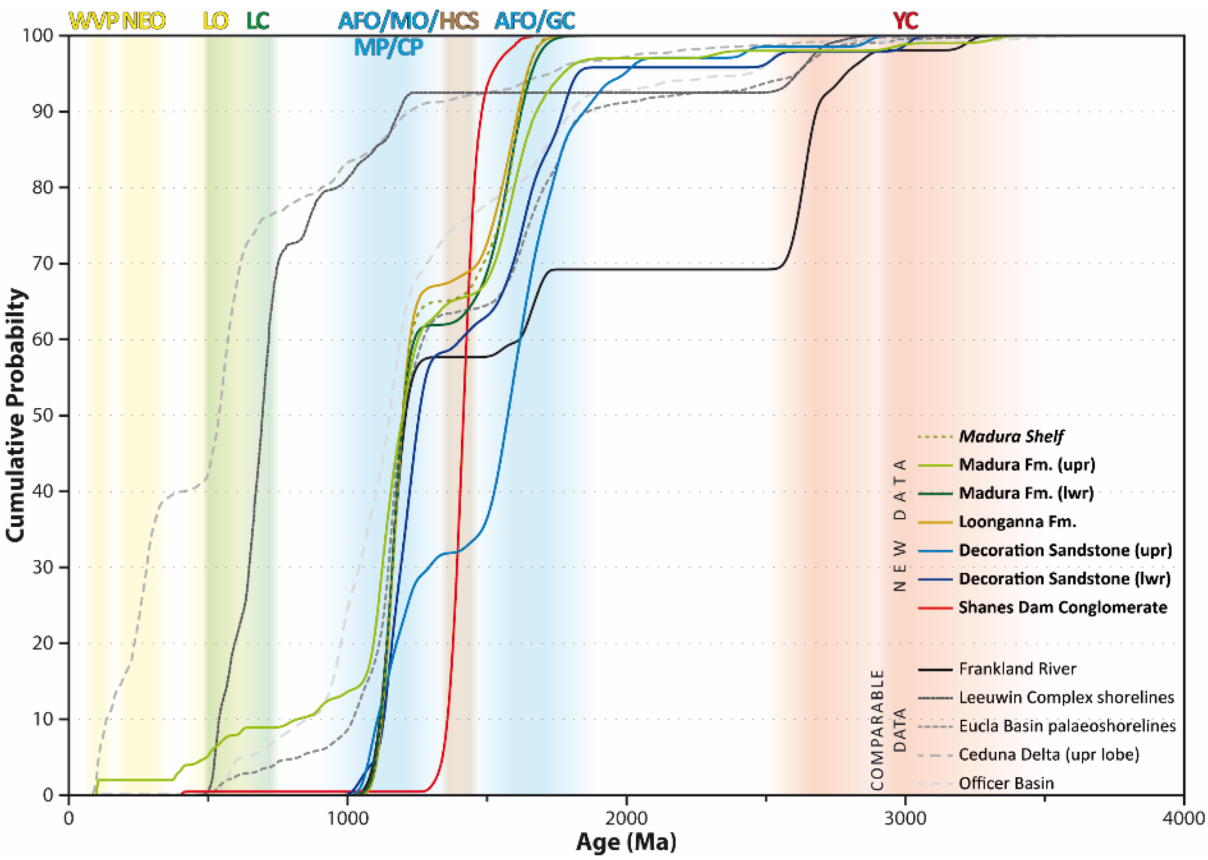

Fig. 5 Cumulative probability plots of detrital zircon age spectra of near-concordant data (<10% discordant) for samples analysed here, as well as comparative sediment reservoirs. Ceduna Delta in eastern Bight Basin (MacDonald et al., 2013), Leeuwin Complex derived material in modern shorelines representing the Pinjarra Orogen (composite dataset from combined Yallingup and Augusta samples; Requilme, 2016; Sircombe and Freeman, 1999), Frankland River sediment draining the Albany-Fraser Orogen (FR3; Cawood et al., 2003), Officer Basin sediments (Bodorkos et al., 2006; Nelson, 1999, 2002a, b, 2004a, b, c; Reid et al., 2013; Wingate and Bodorkos, 2007b, c, d; Wingate et al., 2013), Cenozoic shorelines fringing Eucla Basin (Reid et al., 2013). Coloured vertical bars indicate the significant age signatures of crystalline source regions and may indicate ultimate zircon grain origin when correlated with sudden vertical inflections in a cumulative probability spectrum. WVP – Whitsunday Volcanic Province (Bryan et al., 2012), NEO – New England Orogen and LO – Lachlan Orogen (Veevers et al., 2016; and references therein), LC – Leeuwin Complex of the

Pinjarra Orogen (Collins, 2003), AFO – Albany-Fraser Orogen (Spaggiari et al., 2015), MO – Musgrave Province (Kirkland et al., 2015a), MP – Madura Province and CP – Coompana Province (Fraser and Neumann, 2016; Kirkland et al., 2017), HCS – Haig Cave Supersuite of the Madura Province (Kirkland et al., 2017), GC – Gawler Craton (Kositcin, 2010b), YC – Yilgarn Craton (Nelson, 1997; Veevers et al., 2005).

4.4 Hf-isotope data

All Hafnium isotope data are shown in Fig. 7 and listed in Supplementary Table 5. Two samples from the Madura Formation (199453, 199454) show similar Hf isotopic characteristics, with the exception of a unique <350 Ma zircon population in sample 199453 (Barham et al., 2016). The majority of grains in both samples are Proterozoic and range between depleted mantle (DM) -like to sub-CHUR and scatter around an evolutionary array that tracks back to between 1.5-2.0 Ga along a $^{176}Lu/^{177}Hf$ slope of approximately 0.015 (Fig. 7). The young <350 Ma population in 199453 (upper Madura Formation) sits between CHUR and DM and ranges up to Hf_i = 0.283075 (at 106 Ma; εHf = 12.94). Two stage Hf model ages for both samples are essentially unimodal and peak at c. 1.8 Ga.

One sample of the Loongana Formation (199455) defines a tight evolutionary array along a $^{176}Lu/^{177}Hf$ slope of c. 0.015 that intersects DM at 1.9-2.0 Ga. Essentially all data sit between CHUR and DM, with the most evolved analysis indicating a value Hf_i = 0.281833 at 1576 Ma (εHf = 1.83; Fig. 7).

Two samples from the Decoration Sandstone (199443 and 199444) yield very similar Hf isotopic signatures mainly ranging from CHUR-like to more radiogenic values around DM (Fig. 7). The majority of grains are Proterozoic with values as evolved as Hf_i = 0.281483 (at 1632 Ma; εHf = -9.34) but range to as radiogenic as Hf_i = 0.282445 (at 990 Ma; εHf = 10.34).

A minor subpopulation of Archean grains range between CHUR and somewhat more evolved signatures (0.280864 Hf_i at 2514 Ma; εHf = -11.17). Two stage model ages (assuming a Lu/Hf ratio of 0.015; Griffin et al., 2002) range from c. 1.1 Ga to 3.8 Ga with the majority indicating a model age of c. 1.8 Ga, with a secondary mode at c. 2.6 Ga.

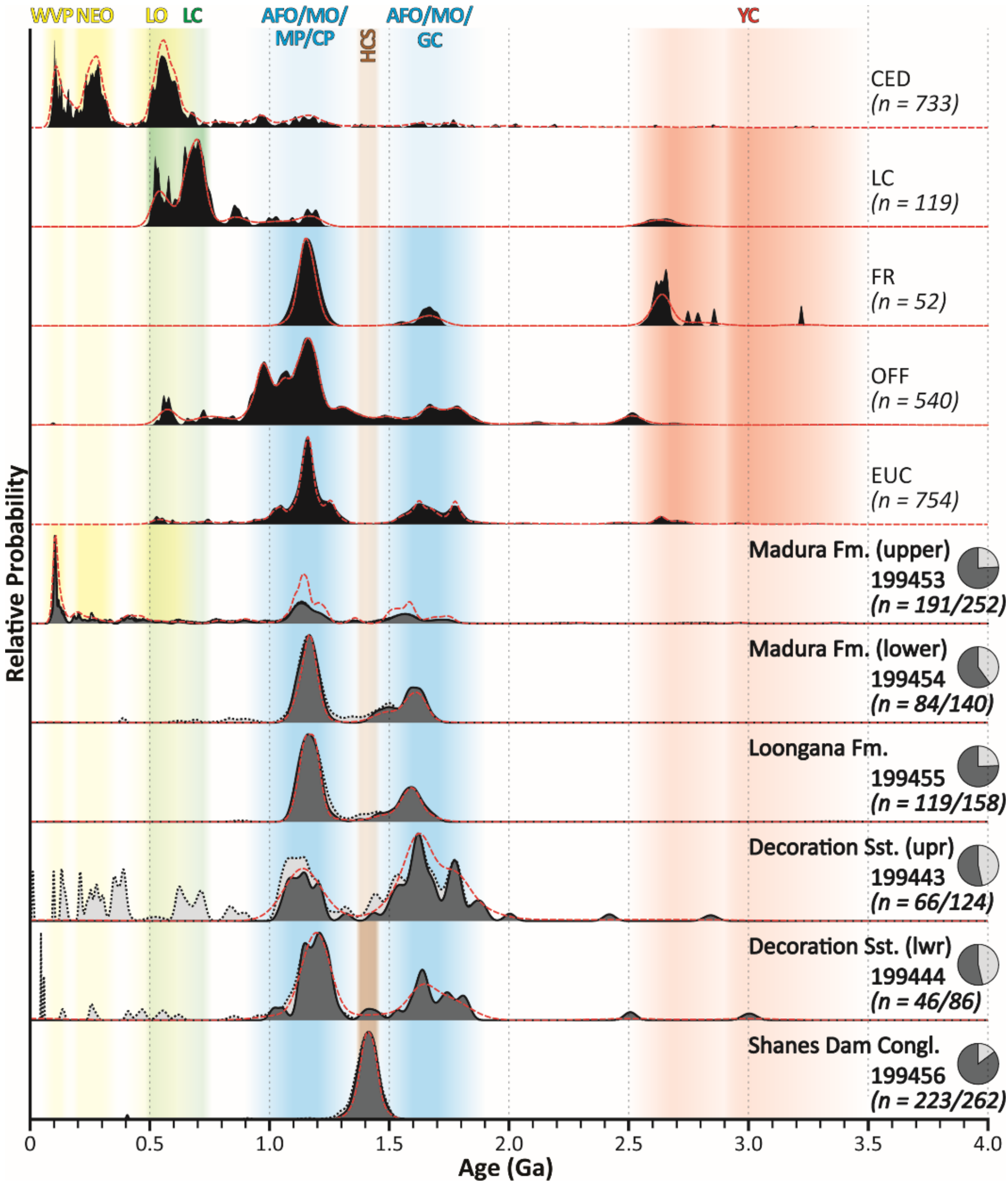

Fig. 6 Stacked plots of detrital zircon age spectra. Red dashed lines represent kernel density estimates of near-concordant data (<10% discordant), grey fill areas represent standard probability density functions (light grey = all age data; dark grey = near-concordant data).

Black plots represent concordant data from published comparable detrital datasets. Pie-charts correspond to the relative proportions of concordant and discordant analyses with colours matching those of the plotted spectra. CED – Ceduna Delta in eastern Bight Basin (MacDonald et al., 2013), LC - Leeuwin Complex derived material (composite dataset from combined Yallingup and Augusta samples; Requilme, 2016; Sircombe and Freeman, 1999), FR – Frankland River sediment draining the Albany-Fraser Orogen (FR3; Cawood et al., 2003), OFF – Officer Basin sediments (Bodorkos et al., 2006; Nelson, 1999, 2002a, b, 2004a, b, c; Reid et al., 2013; Wingate and Bodorkos, 2007b, c, d; Wingate et al., 2013), EUC – Cenozoic shorelines fringing Eucla Basin (Reid et al., 2013). Coloured bars indicate significant age signatures of crystalline source regions. WVP – Whitsunday Volcanic Province (Bryan et al., 2012), NEO – New England Orogen and LO – Lachlan Orogen (Veevers et al., 2016; and references therein), LC – Leeuwin Complex of the Pinjarra Orogen (Collins, 2003), AFO – Albany-Fraser Orogen (Spaggiari et al., 2015), MO – Musgrave Province (Kirkland et al., 2015a), MP – Madura Province and CP – Coompana Province (Fraser and Neumann, 2016; Kirkland et al., 2017), HCS – Haig Cave Supersuite of the Madura Province (Kirkland et al., 2017), GC – Gawler Craton (Kositcin, 2010b), YC – Yilgarn Craton (Nelson, 1997; Veevers et al., 2005).

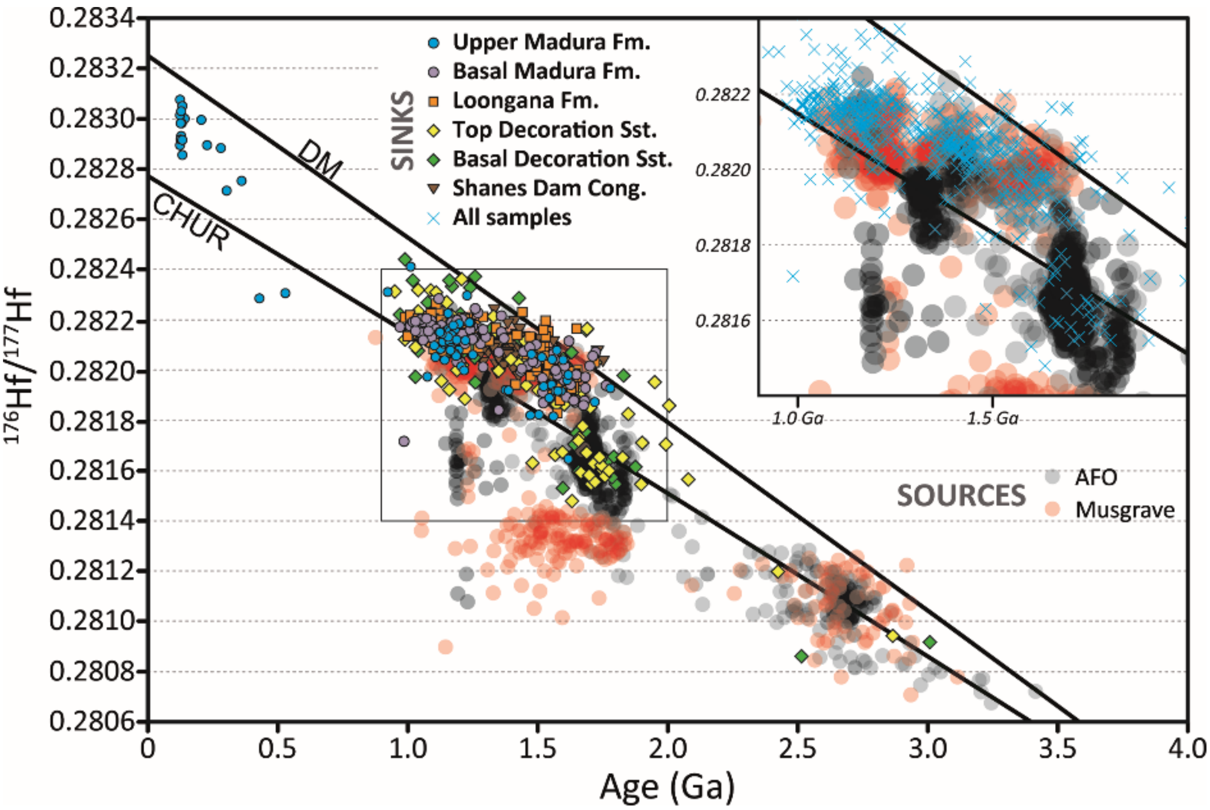

Fig. 7 Hafnium-evolution plot of detrital zircon grains analysed overlain on magmatic zircon data from the Musgrave Province (Kirkland et al., 2015a) and Albany-Fraser Orogen (Spaggiari et al., 2015). Hafnium isotope values calculated at grain crystallisation age. Age and Hf-isotope uncertainty within data points as plotted. DM—depleted mantle; CHUR—chondritic uniform reservoir. Inset shows main detrital populations in more detail with respect to the Hf-isotopic compositions of AFO and Musgrave Province source regions.

Data from Shanes Dam Conglomerate (199456) are relatively clustered and sit between CHUR and DM on an evolutionary diagram (Fig. 7). A best fit line through the dataset lies along a Lu/Hf slope of approximately 0.015 and intersects DM at c. 1.8 Ga. Two of the oldest grains analysed have a DM like composition at 1.8 Ga.

5 DISCUSSION

5.1 Geological significance of Shanes Dam Conglomerate and the Decoration Sandstone

The definition of Shanes Dam Conglomerate and the Decoration Sandstone provide independent evidence of pre-Mesozoic sedimentary systems on the southern margin of Australia.

Despite the polymict nature of Shanes Dam Conglomerate, zircon provenance data demonstrate a surprisingly uni-modal age population centered on 1412 Ma (Fig. 5-6; Supplementary Fig. 3). This detrital zircon populations age is indistinguishable from that of the underlying Haig Cave Supersuite (associated with the Loongana Arc; Spaggiari et al., 2015) basement of the Madura Province dated to 1403-1415 Ma ~40 km to the northeast of HDDH001 in wells LNGD-0001 and LNGD-0002 (metagabbro, metatonalite and amphibolite samples with a mean age of 1409 ± 6 Ma; Kirkland et al., 2013b, c; Nelson, 2005a, b, c; Wingate et al., 2015), and 1389 ± 7 Ma in MAD002, ~20 km to the west (Wingate et al., 2016). This indicates local sediment sourcing from underlying crystalline basement and potential intermediate sedimentary packages (indicated by sedimentary clasts). The significant contribution of Mesoproterozoic zircon grains from a volcanic arc is mirrored regionally in mid-Mesoproterozoic basins in the AFO (Arid Basin; Spaggiari et al., 2015) and correlative geology in Wilkes Land, East Antarctica (metasediments on the Windmill Islands; Morrissey et al., 2017), as well as the Musgrave Orogen (Ramarama Basin; Evins et al., 2012). These data point to an extensive switch to convergence along the boundaries between the West Australian Craton, North Australian Craton and Mawson Craton at this time, with subduction-related arc-volcanism defining basin settings and influencing sediment provenance prior to final cratonic amalgamation.

A single concordant zircon grain with a Devonian age of 407 Ma is an outlier in the detrital zircon age signature, which, assuming it is not disturbed nor a contaminant, provides a maximum depositional age constraint for Shanes Dam Conglomerate. Deposition of Shanes Dam Conglomerate is otherwise temporally constrained by the next youngest concordant zircon age subgroup at 1301 Ma (1300 ± 15 Ma; 1302 ± 16 Ma; Supplementary Fig. 3). Since the conglomeratic unit is significantly ferruginised in places and the disconformity with overlying Madura Shelf units is pronounced, Shanes Dam Conglomerate is considered to significantly pre-date the Mesozoic. Shanes Dam Conglomerate could be equivalent to Devonian units in the Officer Basin. However, if the Devonian grain is not representative of Shanes Dam Conglomerate, the unit may be Mesoproterozoic in age, given the next youngest Mesoproterozoic zircon age constraint and characteristic 1400 Ma detrital zircon population, similar to sediments of this age in the Arid Basin within the Albany-Fraser Orogen (Spaggiari et al., 2015). Lower Permian diamictites correlated to the Wilkinson Range beds and Paterson Formation crop out, or are adjacent in the subsurface to, Madura Shelf stratigraphy, and equivalent late Palaeozoic glacigene rocks are also known to underlie the Bight and Eucla Basins in South Australia (Lowry, 1970). However, a possible glacigene origin for Shanes Dam Conglomerate is not suggested by any core features and the unimodal zircon population indicates a local source, correlating with underlying basement. Instead, the depositional environment of Shanes Dam Conglomerate is inferred based on sedimentology and detrital zircon geochronology to have been a high energy, alluvial-fluvial setting with localised steep topography (Fig. 4) capable of transporting and rounding cobbles and pebbles.

The Decoration Sandstone appears geographically restricted despite its stratigraphic thickness, indicating either that the unit itself developed in a pronounced topographic irregularity or that it is preserved locally due to subsequent down-faulting prior to Mesozoic sedimentation. The absence of “pan-Gondwanan” ~500-700 Ma zircon grains (Fig. 5-6), which are commonly encountered in Officer Basin sediments to the north, as well as wider Palaeozoic Australia (c.f. Haines et al., 2013; Shaanan et al., 2017; Veevers et al., 2006;

2016), suggests either: (i) the Decoration Sandstone pre-dates the generation of this sediment pulse, or (ii) sediment contribution of 500-700 Ma orogenesis decreased towards the southern Officer Basin and were effectively diluted out by AFO and Musgrave Province sources.

Given the interpreted presence of bioturbation in the Decoration Sandstone, similarities in aspects of zircon population age spectra (Fig. 5-6), and basin interpretation from aeromagnetics, the Decoration Sandstone is interpreted as part of the revised southerly Palaeozoic extension of the Officer Basin (Fig. 1; Westwood Shelf; Grey et al., 2005; Haines et al., 2008). The apparent relative textural immaturity of the Decoration Sandstone sediments and differences in the dominant peak ages in the zircon age spectra from Officer Basin sediments (e.g. Lennis Sandstone and Wanna Formation; Haines et al., 2013) suggests a stronger influence of more proximal sediment contributions (i.e. Albany-Fraser Orogen and Musgrave Province) and a sufficiently distal position to reduce the influence of any significant pan-Gondwanan component. This interpretation is supported by similar detrital zircon age spectra signatures in southerly samples from the Officer Basin (Trainor Hill Sandstone and Apamurra Fm.; Reid et al., 2013). The minimum depositional age of the Decoration Sandstone is constrained by its disconformable contact with the overlying Early Cretaceous (Valanginian-Hauterivian *Foraminisporis wonthaggiensis* Zone) Loongana Formation. The Decoration Sandstone was likely deposited in a fluvial to intertidal/coastal environment with an occasional aeolian influence, in an arid climate because of the red-bed colouration. This is evidenced by the cyclical nature of the sandstone, which switched from periods of deposition in a wet environment, characterised by the wavy bioturbated beds, transitioning to sections of planar laminated and cross-stratified sandstones with well rounded, highly spherical quartz that are more characteristic of aeolian sands (Pye and Tsoar, 2009). The formation is capped by a mudrock, which indicates deposition in a low energy environment, and possibly represents a rise in relative base-level. In general, the structure and oxidation state of the irregular bedded sandstone section of the Decoration Sandstone resembles that of the mid-Palaeozoic Wanna Formation of the Officer Basin (Jackson and van de Graaff, 1981), parts of the Silurian-Devonian Mereenie Sandstone of the Amadeus Basin in central Australia (Edgoose, 2013) and Tandalgoo Formation in the Canning Basin of NW Australia (Lehmann, 1984), and the mid-Palaeozoic fluvial-paralic Tumblagooda Sandstone of the Southern Carnarvon Basin (Fig. 1; Hocking, 1991). An early Cambrian age would satisfy (i) the presence of bioturbation, (ii) lack of significant 500-700 Ma detritus (which appears to have become widespread in the Ordovician regionally), (iii) aeolian influence (evidenced widely across southern central Australia in response to the Paterson-Petermann Orogeny, e.g. McFadden and Lungkarta Formations; Grey et al., 2005), and (iv) similarities in detrital zircon spectra with Cambrian fluvial sediments from the Officer Basin (c.f. Durba Sandstone - Wingate and Bodorkos, 2007a).

5.2 Palaeotopography and Mesozoic evolution of the Madura Shelf and southern margin of Australia

Overall, there is a gentle, broadly southerly dip across the basement surface towards the central, deepest wells of Eyre 1 and Madura 1 (the latter drilled to -535 m AHD without encountering basement; Fig. 4). Although data constraints are sparsely distributed, the magnitude of apparent dip varies from an essentially flat >0.2° (~450 m drop over ~200 km between MAD014 and Madura 1) to a more locally variable 2° (a change of ~60 m over 1.8 km between SDDH002 and SDDH001). Eucla 1 intersected basement at -201 m (AHD), higher than other coastal wells and up-slope from other wells to the north, against the regional trend (Fig. 4).

Mesozoic sedimentation on the southern margin Bight Basin is recorded from at least the late Jurassic in presently offshore half-graben structures (e.g. Jerboa 1, Eyre Sub-basin - Totterdell et al., 2000), which formed in a series of west to east propagating rifts (Blevin and Cathro, 2008; Totterdell and Bradshaw, 2004). However, by the early Cretaceous, more regional thermal subsidence is evidenced by deposition of the Loongana Formation (dated via palynology as Valanginian-Hauterivian; ~140-130 Ma), which corresponds to Valanginian to mid-Albian (~140-100 Ma) fluvio-lacustrine sediments of the Bronze Whaler Supersequence interpreted in offshore basins (Bradshaw et al., 2003; Totterdell et al., 2000). Penecontemporaneous sedimentation began in low lying areas, including the central SDDH/HDDH boreholes and Madura 1 area, and further east in the FOR010/011/014 and Albala-Karoo wells (Figs. 3, 4, 8). Variations in the thickness and spatial development of basal clastics in the region imply some topographic control on sedimentation. However, given the relatively minor nature of thickness variations (tens of metres in the Loongana Formation) over the extensive area, and later regional shared sedimentation, pre-Cretaceous landscape planation/denudation is inferred (Fig. 4a). The high-energy fluvio-lacustrine coarse-grained clastic facies of the Loongana Formation are poorly sorted and texturally immature, suggesting rapid deposition and limited reworking.

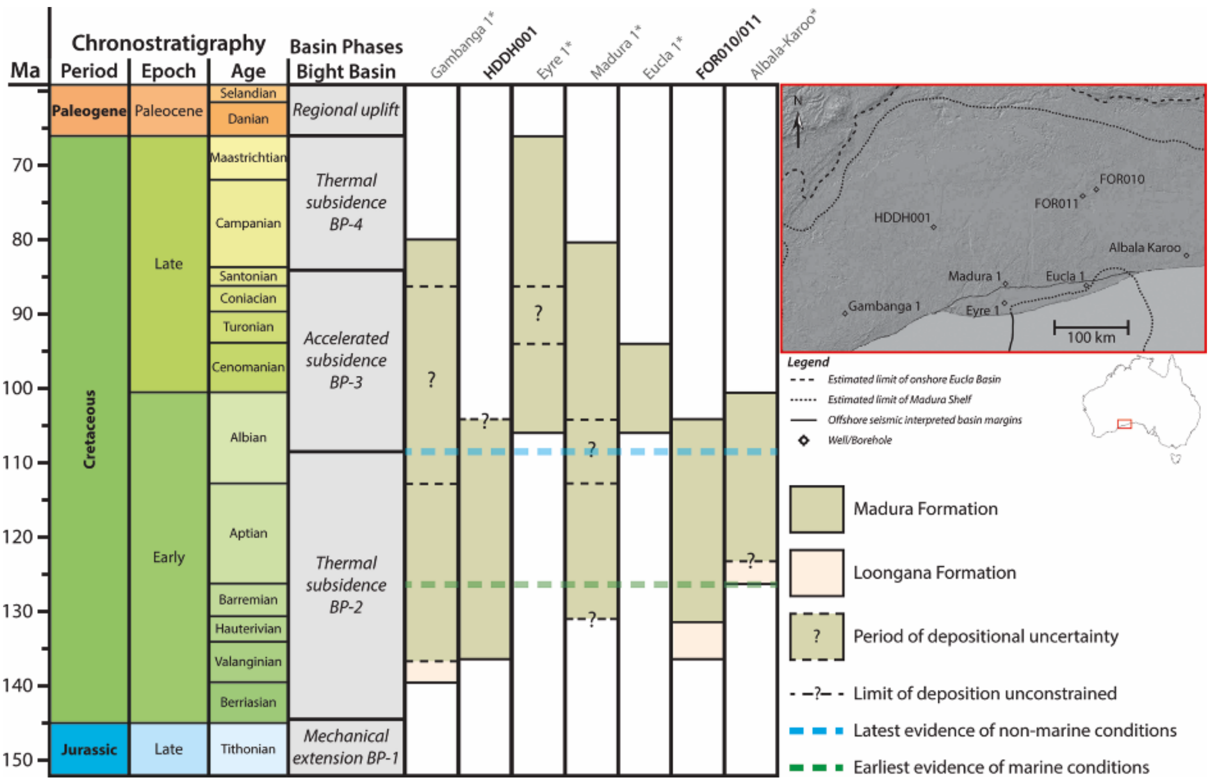

*Fig. 8 palynologically constrained (Supplementary Table 2) timing of sedimentation on the Mesozoic Madura Shelf. Basin phases adapted from Totterdell et al. (2000). Additional palynostratigraphical constraints from wells marked with an * derived from Totterdell and Krassay (2003).*

Continued thermal subsidence in the Cretaceous led to more widespread deposition of finer sediments of the Madura Formation (Fig. 4b). Algal palynomorphs suggest that freshwater-brackish conditions continued through from the Loongana Formation into the basal Madura Formation (*Foraminisporis wonthaggiensis* Zone). Total organic carbon data near the base of the Madura Formation in Gambanga 1 also suggest a non-marine influence (Totterdell and Krassay, 2003). Thin charcoal beds are especially concentrated in the Loongana Formation and at the base of the Madura Formation (Supplementary Fig. 1-2) and suggests that the Cretaceous catchment surrounding the Madura Shelf, or localised topographic highs, were vegetated and subjected to occasionally significant fire events (c.f. Nichols and Jones, 1992). Although the Madura Formation was initially deposited under freshwater conditions, the presence of glauconite in some wells (FOR011, HDDH002 and SDDH002) demonstrates at least intermittent marine conditions at or near the base of the formation. Lithological (glauconite, progressive dominance of finer grain size) and macrofaunal (incursion of pelagic cephalopods) indicators concur with palaeoenvironmental reconstructions based on marine dinocysts, that marine conditions became fully established on the Madura Shelf by the mid-Cretaceous (Mid-Albian to Maastrichtian; ~110-66 Ma; Fig. 8). This was during a period of accelerated subsidence and a global eustatic high that saw similar marine conditions established across the Bight Basin (mid-Albian to Cenomanian Blue Whale Supersequence; Blevin and Cathro, 2008; Bradshaw et al., 2003; Cloetingh and Haq, 2015; Totterdell et al., 2000). The exact timing of the transgression across the Madura Shelf is uncertain – it may predate the mid-Albian since the palynology sample from the upper Madura Formation (FOR011) overlies ~80 m of glauconitic siltstone.

Across most of the Madura Shelf, palynology indicates initiation of sedimentation in the -Barremian-Valanginian (~145-133 Ma; Fig. 8; Section 4.2). However, in Eyre 1 and Eucla 1, deposition appears to have commenced much later, in the Albian (Totterdell and Krassay, 2003). The Madura Formation is relatively thin in Eucla 1, which is situated on, or adjacent to, a relative basement high just inboard of a region interpreted from seismic profiles to have elevated basement and an associated thin or absent Mesozoic sequence (Fig. 4 & 8; Bradshaw et al., 2003; JNOC, 1992). Since Eucla 1 lacks typical non-marine strata (Loongana Formation and lower Madura Formation) at the base of the Cretaceous sequence, this area is interpreted as a palaeohigh that was simply inundated later than elsewhere. However, unlike Eucla 1, the sequence in Eyre 1 is relatively thick, with one of the deepest basement contacts (Fig. 4 & 8), and thus, a delayed transgression of higher ground requires that the area subsequently experienced enhanced subsidence relative to surrounding areas. Late-stage subsidence is supported by the apparent continuation of sedimentation in the well beyond that experienced in other wells (Fig. 8; Maastrichtian vs. Cenomanian commonly elsewhere; ~66 Ma vs. ~105 Ma). Graben-like structures have been identified in 2D seismic shot across the offshore Bight Basin, which are orientated north-northeasterly from the main east-west sub-basin trend towards the area of Madura 1 and Eyre 1 (Fig. 4; Bradshaw et al., 2003; JNOC, 1992; Totterdell and Krassay, 2003). Onshore fault-related localised subsidence may be supported by recent onshore passive seismic, which suggests significant basement depth changes in the area (Scheib et al., 2016). The identification of this faulting, much later than the typical mechanical rift phase of the Bight Basin, has implications for the subsidence temporal framework of the southern Australian margin, as well as interpretation of the timing of faults and fault-affected depositional packages in seismics offshore that are poorly constrained by well ties.

At the termination of sedimentation, the Madura Formation had largely blanketed pre-existing topography, leaving a relatively flat surface with only a slight north-south slope that is remarkably consistent across the region (~0.1° based on contouring of well constraints), essentially equivalent to that of the modern continental shelf and parallel to the modern shoreline (Fig. 4). At the end of the Cretaceous, the Madura Shelf experienced an interval of regional uplift that effectively marked the end of Mesozoic sedimentation and led to a period of prolonged exposure for several tens of millions of years prior to the Eocene onset of carbonate sedimentation across the Eucla Basin (Clarke et al., 2003; Hou et al., 2011; Lowry, 1970; MacDonald et al., 2013; Totterdell and Krassay, 2003). Despite this hiatus, very little evidence for prolonged exposure and denudation is preserved. Well BN1 (Fig. 4b) presents the only significant anomaly in the surface elevation of the Madura Formation, being some 100 m lower than in surrounding wells. Given that the basement depth is relatively consistent in this area, and the formation is relatively thin in BN1, the lower elevation is interpreted to represent localised erosion.

Present-day elevation differentials across raised Cenozoic palaeoshoreline features fringing the Cenozoic Eucla Basin demonstrate significant uplift differences have developed across the region since at least the Miocene (Fig. 1; Hou et al., 2008; Sandiford, 2007). Patterns of uplift, as well as the geographical migration of depocenters through time, disparities in the width of the continental shelf around Australia and upstream migration of nick points in river profiles draining the Australian continent, have all been discussed in terms of the drift of the Australian Plate over mantle buoyancy irregularities, i.e. dynamic topography (Barnett-Moore et al., 2014; Czarnota et al., 2013; Müller et al., 2016; Quigley et al., 2010; Sandiford, 2007; Schellart and Spakman, 2015). Since the Cretaceous, the Australian Plate has interacted with both positive and negative mantle buoyancy anomalies associated with spreading between Australia and Antarctica as well as subduction along the northern margin of Australia and ancient crustal slabs that were over-ridden as the Australian Plate moved rapidly north (Czarnota et al., 2013; 2014). Although many finer details are still unclear, it has been suggested that a substantial part of the uplift experienced in SW Australia through the later Cenozoic relates to migration away from a dynamic topography low associated with an ancient subducted slab (Barnett-Moore et al., 2014). The apparent absence of any E-W elevation differential on the surface of the Madura Formation suggests that the Madura Formation was entirely deposited prior to the later, probable Eocence subsidence associated with the dynamic topographic low responsible for the development of the Eucla Group carbonates and later tilting of Cenozoic palaeoshorelines. Subsequently, exiting the dynamic topographic low has returned the Madura to its pre-existing state, while the Cenozoic carbonate sequence has been uplifted to different degrees dependent on original position within the dynamic topographic low.

5.3 Zircon provenance and implications for source region denudation

5.3.1 c. 1650 Ma (~1500-1800 Ma) grains

Detrital zircon grains of this age constitute the dominant age peak for sample 199443 – the upper Decoration Sandstone and secondary peak in the age spectra of samples 199444, 199453, 199454 and 199455, spanning the Decoration Sandstone (lower), Loongana Formation and the Madura Formation.

Underlying the Madura Shelf through eastern regions (Forrest Zone of the Coompana Province; Fig. 1) are c. 1610 Ma granites and monzodiorite (Toolgana Supersuite - Kirkland et al., 2017). Further west, magmatism associated with the 1710-1650 Ma Biranup Orogeny of the Albany-Fraser Orogen (Spaggiari et al., 2014; 2015) also constitutes a potential source region for this zircon population age peak. Further north, the Warlawurra Supersuite in the western Musgrave Province has been dated to 1607-1583 Ma (de Gromard et al., 2016), whilst through the central and eastern Musgrave Province, basement ages range from 1665 to 1540 Ma (de Gromard et al., 2016; Edgoose et al., 2004; Jagodzinski and Dutch, 2013). However, there is a paucity of grains of this age in most Officer Basin samples between the Madura Shelf and Musgrave Province (Fig. 5-6; Haines et al., 2013; Reid et al., 2013).

Younger components of the c. 1650 Ma zircon age spectrum peak could represent sub-populations derived from the central Gawler regions of the Gawler Range Volcanics (c. 1590 Ma), Hiltaba Suite (c. 1590 Ma) and St. Peter Suite (c. 1620 Ma) (Belousova et al., 2009; Reid et al., 2014). However, the lack of other distinctive Palaeoproterozoic peaks in the age spectra (c. 1740, 1850, 2020 and 2500 Ma; Belousova et al., 2009) of the samples analysed herein, argues against derivation of material from the east.

5.3.2 c. 1400 Ma grains

The grains of a c. 1400 Ma age that dominate sample 199456 (Shanes Dam Conglomerate in HDDH001) correspond with zircon crystals with juvenile Hf-signatures (Hf_i = ~0.2820-0.2822 at ~1400 Ma; εHf = ~3.5-11.0) in the Haig Cave Supersuite basement of the Madura Province (representing the "Loongana Arc"; Spaggiari et al., 2015) with a mean age of 1409 ± 6 Ma (Wingate et al., 2015). Hafnium isotopic characteristics of these zircon grains are similar to those formed in parts of the Musgrave Province at this time and point to similarities in geological evolution (Fig. 7; Kirkland et al., 2017). Essentially contemporaneous sedimentation in the Arid Basin (eastern AFO; Fig. 1) preserves detrital zircon grains with a pronounced 1425-1375 Ma age spectrum peak, implicating erosion of the oceanic "Loongana Arc" into adjacent depocentres during the Mesoproterozoic (Spaggiari et al., 2014; 2015).

5.3.3 c. 1150 Ma (~1000-1300 Ma; Grenville) grains

Zircon grains of 1300-1000 Ma age represent the dominant peak in the detrital zircon age spectra for samples 199444, 199453, 199454 and 199455, spanning the lower Decoration Sandstone, Loongana Formation and the Madura Formation, and the secondary peak for sample 199443 – the upper Decoration Sandstone. A number of "Grenvillian" rock-forming events in potential source regions match these ages (Clarke et al., 1995). Crystalline rocks of the Moodini Supersuite are found throughout the eastern Madura Province and across the Coompana Province beneath the Madura Shelf and ranges in age from 1181-1125 Ma (Fig. 1; Neumann and Fraser, 2016; Wingate et al., 2015). Further north, metamorphism and widespread felsic intrusions occurred from c. 1220-1150 Ma during the Musgrave Orogeny (Edgoose et al., 2004; Jagodzinski and Dutch, 2013; Kirkland et al., 2015a). To the west, from 1200-1140 Ma, the Esperance Supersuite was intruded during Stage II of the Albany-Fraser Orogen (Clark et al., 2000; Spaggiari et al., 2014).

A compilation of detrital zircon data from across the Gawler Craton to the east of the study area shows a significant peak in the age spectrum at 1169±48 Ma that does not match any known magmatic or metamorphic events in the Gawler Craton (Belousova et al., 2009). Given the widespread distribution of this sub-population across the Gawler Craton, Belousova et al. (2009) argued that these data indicate the presence of unrecognized sources of this age within the craton itself. However, based on new data from basement beneath the Nullarbor Plain, a more plausible explanation of their occurrence, age and relatively juvenile Hf-signatures (Kirkland et al., 2017) appears to be shedding of material from the Moodini Supersuite, in the Coompana and Madura Provinces (Fig. 1).

5.3.4 c. 106 Ma grains

Sample 199453 from the upper Madura Formation (FOR011) yielded 28 grains contributing to the c. 106 Ma sub-population. This sample is stratigraphically proximal to a palynological sample (Fig. 3) containing a diagnostic assemblage attributed to the *Pseudoceratium* [*Endoceratium*] *ludbrookiae* zone of Helby et al. (1987), which ranges from c. 104 to 107.5 Ma. Microscopic investigation of the zircon grains in this sub-population demonstrate preservation of euhedral form and distinctive oscillatory zoning indicative of growth in a magma chamber (Barham et al., 2016). The mid-Cretaceous age, more radiogenic Hf-isotope characteristics and light rare-earth element depleted characteristics of these zircon grains are all consistent with the broader eastern Gondwanan siliceous large igneous province defined by Bryan et al. (2012) that formed preceding Zealandia-Australia separation (Barham et al., 2016).

5.4 Evolution of sediment routing

5.4.1 Cratonic planation

The absence of typical Yilgarn-aged (~2.6 Ga) zircon grains in samples analysed, or in reference samples from the underlying Officer Basin (Fig. 5-6; Haines et al., 2013; Reid et al., 2013), informs aspects of palaeodrainage patterns in the west of the study region. The potential for the Albany-Fraser Orogen to have acted as a physical barrier to sedimentation from the Yilgarn Craton toward the study region may be significant through much of the Proterozoic history of the Officer Basin. However, comparisons with Palaeozoic palaeovalleys in the Northern Territory and mapping of Yilgarn Craton palaeovalleys and their hosted sediments demonstrates a protracted (at least Mesozoic) history of drainage (Bell et al., 2012; de Broekert and Sandiford, 2005) that would have facilitated detrital grain transfer to the Madura Shelf even with reported tectonically induced reversals and adjustments to drainage patterns during separation of Australia and Antarctica (Beard, 1999; Hou et al., 2008). Therefore, the paucity of Archean grains supports hypotheses (Cawood and Nemchin, 2000; Sircombe and Freeman, 1999) of a denuded Yilgarn Craton landscape lacking sufficient topography to generate a significant supply of detrital zircon grains from at least the Mesozoic.

5.4.2 Stabilised sediment sourcing and recycling

Similarities are apparent in the broadly bimodal detrital zircon age spectra of samples analysed herein and sediment from Cenozoic shorelines and fringing palaeovalleys, modern streams draining the AFO as well as parts of the Officer Basin (Fig. 5-6 & 9). These similarities and parallels in Hf-isotope character, which match magmatic events in the Albany-Fraser Orogen and Musgrave Province (Fig. 7), suggest the Decoration Sandstone and sediments of the Madura Shelf were sourced predominantly from these orogens either directly or secondarily (principally via the Officer Basin), given known drainage and longshore-drift sediment routing pathways (Hou et al., 2011; Reid et al., 2013). However, nuances in the abundance and absolute age of principal components in the zircon age spectra and Hf-isotopic values inform temporal variability in the dominant inputs of detritus into this recycled southern margin sediment pool. The Decoration Sandstone shows sourcing of 1600-1800 Ma zircon from the AFO, specifically two peaks in the zircon age spectra whose ages (~1.65 and 1.8 Ga) and more evolved Hf isotopic values (relative to Madura Shelf samples) suggest derivation from the Biranup and eastern Nornalup Zones of the Albany-Fraser Orogen (Fig. 5-7; Spaggiari et al., 2014). Significant contributions of late Mesoproterozoic (~1.3-1.0 Ga) zircon grains are recognised across the Officer Basin and wider central Australian basins, which are attributed to derivation from the Musgrave Province (e.g., Haines et al., 2016; Reid et al., 2013). Similarly, the more juvenile Hf-character and age of ~1.3-1.0 Ga detrital zircon grains in the Decoration Sandstone are here attributed to derivation from the Musgrave Province.

Mesoproterozoic c.1400 Ma zircon grains are a barely perceptible or negligible component in all but one sample studied (Shanes Dam Conglomerate – 199456), despite basement of this age underlying parts of the Madura Shelf. This indicates a paucity of sediment supply from the underlying Madura and Coompana Provinces, and therefore likely complete planation of pre-existing topography. Consequently, although basement with similar ages to the AFO and Musgrave Province exist in the Madura and Coompana Provinces beneath the study area, what little sediment may have derived directly from underlying crystalline sources was likely diluted by more significant direct and recycled source regions of the AFO and Musgrave Province prior to the deposition of the Decoration Sandstone, Madura Shelf and broader Bight Basin. This, combined with difficulties associated with recycling material from the Coompana and Madura Provinces into upstream palleovalleys that record the characteristic age peaks discussed, as well as reconciling the sheer quantity of sediment preserved, argue against substantial derivation of material from these basement regions into the peak c. 1150 and 1650 Ma zircon sub-populations.

A slightly younger shift in the sub-population age, coupled with more juvenile Hf-isotope signatures, indicates a different source for the majority of detrital zircon grains from the Madura Shelf in the c. 1650 Ma age peak, and infer a greater input from the Musgrave Province than the AFO (Fig. 5-7). The Hf isotopic signature of the zircon detritus charts an evolutionary pattern that strongly resembles that recorded in basement rocks of the region; that is both the Madura and Coompana Provinces (Kirkland et al., 2017), and the juvenile magmatic component of the Musgrave Province that appears to have been extracted from the mantle at c. 1.9 Ga and then been repeatedly refertilized by mantle addition from c. 1.7 Ga until at least c. 1.4 Ga (Kirkland et al., 2015a). This evolutionary pattern contrasts strongly with that seen in the Albany-Fraser Orogen where much of the magmatic record is more evolved, especially in the period 1.4 to 1.8 Ga when Albany-Fraser magmatism also incorporated progressively greater amounts of Archean Yilgarn crust. Unfortunately, overlap in the age and Hf-isotope character of zircon grains from the AFO and Musgrave Province complicates their distinction as potential sources for the c. 1150 Ma zircon age peak identified. Similarities of the detrital zircon age spectra recognised here and those of modern stream sediments draining the Yilgarn and western AFO (Cawood et al., 2003) suggest a dominant AFO sourcing over similar aged Musgrave sources (Fig. 5,6 & 9). However, the more juvenile Hf-isotopic character of the Madura Shelf detrital zircon grains is more similar to 1100-1200 Ma zircon grains from the Musgrave Province rather than more evolved AFO sources that have been characterised (Fig. 7).

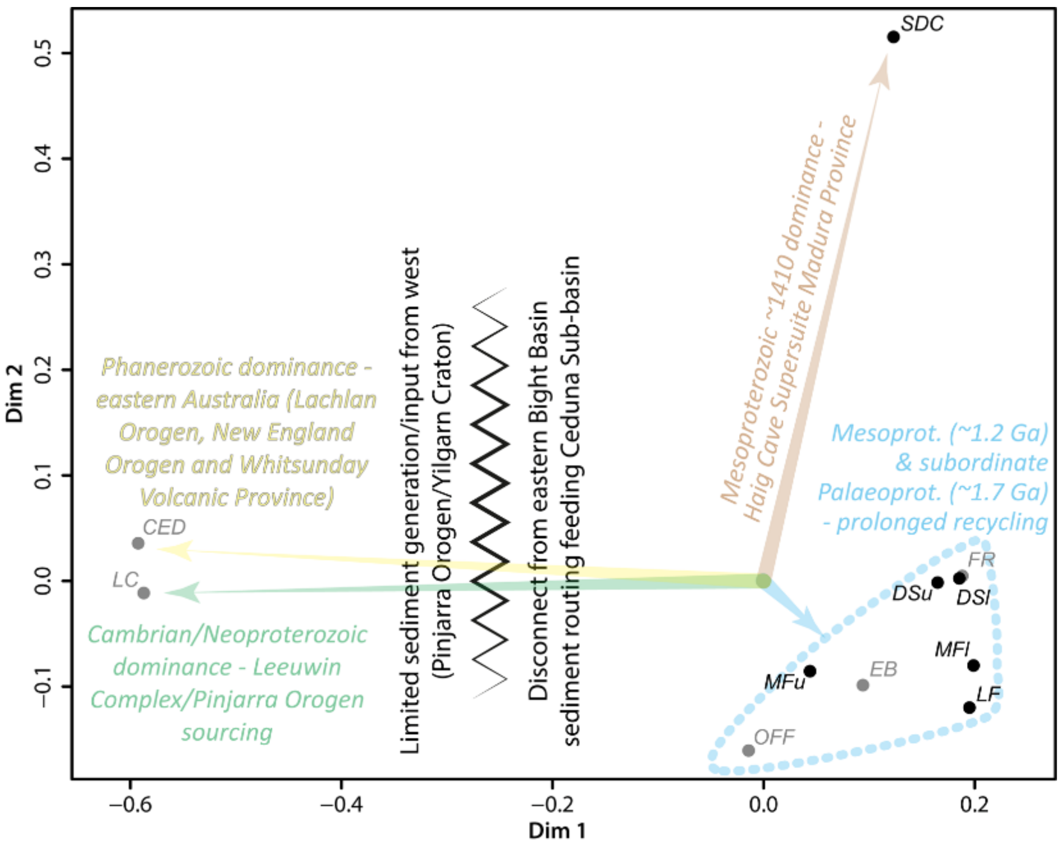

Fig. 9 Kolmogorov–Smirnov based multi-dimensional-scaling plot of detrital zircon sample age dissimilarities (conducted using the statistical software package "provenance" in R; Vermeesch, 2013; Vermeesch et al., 2016). Data have been classically scaled to enable the dissimilarities of the Mesoproterozoic and Palaeoproterozoic dominated samples to be resolved, with increasing distance between sample points indicating greater distinction of detrital zircon population age characteristics. Medium grey points refer to comparable sedimentary datasets. LC - Leeuwin Complex derived material (composite dataset from combined Yallingup and Augusta samples; Requilme, 2016; Sircombe and Freeman, 1999), CED – Ceduna Delta in eastern Bight Basin (MacDonald et al., 2013), FR – Frankland River sediment draining the Albany-Fraser Orogen (FR3; Cawood et al., 2003), EB – Cenozoic shorelines fringing Eucla Basin (Reid et al., 2013), OFF – Officer Basin sediments (Bodorkos et al., 2006; Nelson, 1999, 2002a, b, 2004a, b, c; Reid et al., 2013; Wingate and Bodorkos, 2007b, c, d; Wingate et al., 2013). DSl – Decoration Sandstone lower (199444), DSu –

Decoration Sandstone upper (199443), LF – Loongana Formation (199455), MFl – Madura Formation lower (199454), MFu – Madura Formation upper (199453), SDC – Shanes Dam Conglomerate (199456).

5.4.3 Isolation of sediment systems

Large volumes of early-mid Cretaceous volcanic-derived and subsequently fluvially transported detritus have been reported from the Eromanga Basin (Tucker et al., 2016) across northeastern Australia and even as far as the Upper Cretaceous Ceduna Delta in the eastern Bight Basin on Australia's southern margin (Fig. 1 & 5-6; Lloyd et al., 2016; MacDonald et al., 2013; Veevers et al., 2016). Although interpretations differ on the final scale of the drainage system and the degree of local sediment recycling, U/Pb geochronology and Hf-isotope data from detrital zircon grains from Santonian-Maastrichtian (~86-66 Ma) sediments of the Ceduna Delta indicate substantial ultimate sourcing of material from eastern Australia, with several distinctly different characteristic zircon populations to those that have been identified on the Madura Shelf. Comparisons of detrital zircon age spectra show that the main c. 1150 Ma and c. 1600 Ma age peaks from the Madura Shelf samples are negligible in the Ceduna Delta, and the main Ceduna Delta lobe age peaks of c. 200-300 Ma and c. 500-700 Ma are essentially absent in the Madura Shelf samples (Fig. 5-6 & 9). These differences suggest that erosion of the Madura Shelf was unlikely to have been a major contributor of sediment to the younger Ceduna Delta. Furthermore, the mid-Cretaceous zircon sub-population shared between the Ceduna Delta and upper Madura Formation appears unlikely to have been delivered by related transport systems (Barham et al., 2016). In the Madura Formation sample, the pristine nature of the zircon grains, their stratigraphic definition/isolation and the synchroneity of zircon age peak and palynological age, all argue against typical aeolian, fluvial, alluvial or marine transportation. These data led Barham et al.

(2016) to conclude that the c. 106 Ma volcanic zircon grains had been rapidly and significantly transported with little modification in an eruptive cloud from violent explosive eruptions around the Whitsundays and incorporated into the catchment of sediments at this level on the Madura Shelf. Alternatively, these Phanerozoic components could represent a short-lived Ceduna precursor connection between the Eromanga Basin and Madura Shelf in the Albian. The grain characteristics, palynology and dominance of the youngest zircon age component would then suggest limited transport of extremely distal eruption products quite distinct from the eventual large-scale sediment routing that later supplied the Ceduna Delta and also contributed a variety of other east-coast zircon signatures. Interestingly, detrital zircon age spectra from a Cenozoic palaeovalley draining into the eastern onshore Eucla Basin, have a distinct eastern Australia signature mixed more thoroughly with local crystalline sources (Reid et al., 2009). Ultimately though, a precursor south coast connection from the Eromanga Basin supplying the Madura Shelf would require very dramatic reconfiguration and broadening of the source region, acceleration of erosion across parts of northeastern Australia during the mid-Cretaceous, and significant redirected channelling of sediment to form the Ceduna Delta. Proposed regional reworking of Permian to Early Cretaceous sediments into the Ceduna Delta (MacDonald et al., 2013) would suggest greater similarities of the Madura Shelf and Ceduna Delta zircon spectra should be expected if these two systems shared localised sediment routing systems. However, the distinctiveness of the systems is instead interpreted as the Ceduna Sub-basin and Madura Shelf being largely decoupled in sediment supply systems (Fig. 9), with eastern Madura Shelf sediments also reportedly expressing similar detrital zircon age spectra to that reported here for the Loongana Formation (Bendall et al., 2016). The temporally defined nature of the eastern Australian detritus in the Ceduna Sub-basin of the Bight, distinct from slightly older Madura Shelf sediments, as well as later Cenozoic shoreline detritus, agrees with modelling of eastern

Australian driving a temporally defined sediment pulse across the Eromanga Basin and ultimately into the Ceduna Delta (Müller et al., 2016). With interruption of this uplift and reorganisation of drainage pathways, central southern Australian sediment routing systems returned to a disconnected state from those of eastern Australia.

Westerly longshore drift has been argued as significantly affecting sediment derivation and distribution of paleoshorelines through the Cenozoic of the Eucla Basin (Fig. 1), with minor sediment even suggested as deriving from the Pinjarra Orogen (likely the Leeuwin Complex) on the western margin of WA (Hou et al., 2011; Reid et al., 2013). The lack of detritus of this nature recorded in the samples analysed herein suggests that such coastal-driven sediment transport was not significant for any of the units analysed, probably as a result of a limited seaway in the case of the Mesozoic units (Fig. 5-6 & 9). Recycling of the existing sediment reservoir and continued sourcing from the AFO and Musgrave Province would have diluted out any small amounts of western margin sediment that may have been delivered, effectively isolating the Madura Shelf and underlying sequences from western margin crystalline sediment routing systems, which instead were focussed into rift-basins between India and Australia (e.g. Perth Basin, Fig. 1; Cawood and Nemchin, 2000).

6 CONCLUSIONS

The recognition of the Shanes Dam Conglomerate and the Decoration Sandstone under the Madura Shelf highlights an older sedimentary history on the southern margin than previously recognised. Likely Proterozoic erosion caused denudation of the Loongana Arc and other palaeotopography across the Madura and Coompana Provinces, as evidenced by the restriction of the c. 1400 Ma detrital zircon component to the Shanes Dam Conglomerate and Arid Basin succession in the AFO. The Decoration Sandstone is interpreted as a southerly Palaeozoic extension of the Officer Basin (Westwood Shelf) preserved in a relatively localised fault structure or depocenter. These greater stratigraphic complexities identified in the new drillcore are likely a conservative reflection of reality given the relative paucity of stratigraphic drilling in the vast region. However, as well as Cretaceous late-stage fault-subsidence of the Madura Formation inferred from palynology, these new stratigraphic details have significant implications for ongoing resource exploration onshore in terms of determining depth to potential mineralised basement (Scheib et al., 2016), as well as the interpretation of seismic units and structural histories in the offshore Bight Basin.

Despite overlaps in magmatic ages and Hf-isotope systematics of zircon grains from the Madura and Coompana Provinces with the detritus analysed here, data suggest that the majority of sediment in the Decoration Sandstone and Madura Shelf was supplied from the Albany-Fraser Orogen (Biranup and Nornalup Zones) and Musgrave Province. Consistencies in the detrital zircon characteristics throughout various sediment reservoirs in the region suggest prolonged stability of the sediment reservoir in the Phanerozoic.

During the Early Cretaceous, fluvio-lacustrine sedimentation dominated the weak topography of the Madura Shelf. By the mid-Albian, widespread marine conditions had become established, which led to complete blanketing of the region and almost complete concealment of any pre-existing topography by the end Cretaceous and termination of the Madura Formation sedimentation. Although widespread similarities in the evolution of depositional environments across the Bight Basin are recognised between offshore and onshore stratigraphy, substantial differences exist between the detrital zircon character of the northern Bight Basin (Madura Shelf), and the distinct Ceduna Delta in the east. These differences imply a sedimentary disconnect between the eastern Bight Basin and Madura Shelf, and that a relatively temporally distinct and compositionally unique sediment routing system rapidly developed in the eastern Bight Basin by at least the Upper Cretaceous in response to uplift of Australia’s eastern margin.

ACKNOWLEDGMENTS

The authors are grateful to Uri Shaanan, an anonymous reviewer and the handling editor Alan Collins for comments that improved this manuscript. SR would like to acknowledge receipt of an MRIWA Odwyn Jones Award and a Chevron Student Scholarship. Cathylee O'Toole and Elaine Miller are thanked for assistance with sample processing and imaging, respectively. Catherine Spaggiari, Andreas Scheib and Lena Hancock are thanked for support of SR during his studies, which contributed to this project. GeoHistory Facility instruments were funded via an Australian Geophysical Observing System grant provided to AuScope Pty Ltd. by the AQ44 Australian Education Investment Fund program. The authors acknowledge the use of the John de Laeter Center Microscopy & Microanalysis Facility, Curtin University, whose instrumentation has been partially funded by the University, State and Commonwealth Governments. HJA, PWH, and RMH publish with permission of the Executive Director, Geological Survey of Western Australia.

REFERENCES CITED

Barham, M., Kirkland, C.L., Reynolds, S., O'Leary, M.J., Evans, N.J., Allen, H., Haines, P.W., Hocking, R.M., McDonald, B.J., Belousova, E., Goodall, J., 2016. The answers are blowin' in the wind: Ultra-distal ashfall zircons, indicators of Cretaceous super-eruptions in eastern Gondwana. Geology 44, 643-646.

Barnett-Moore, N., Flament, N., Heine, C., Butterworth, N., Müller, R.D., 2014. Cenozoic uplift of south Western Australia as constrained by river profiles. Tectonophysics 622, 186-197.

Beard, J.S., 1999. Evolution of the river systems of the south-west drainage division, Western Australia. Journal of the Royal Society of Western Australia 82, 147-164.

Bell, J.G., Kilgour, P.L., English, P.M., Woodgate, M.F., Lewis, S.J., Wischusen, J.D.H., 2012. WASANT Palaeovalley Map – Distribution of Palaeovalleys in Arid and Semi-arid WA-SA-NT, First Edition ed. Geoscience Australia Thematic Map (Geocat № 73980).

Belousova, E.A., Reid, A.J., Griffin, W.L., O'Reilly, S.Y., 2009. Rejuvenation vs. recycling of Archean crust in the Gawler Craton, South Australia: Evidence from U–Pb and Hf isotopes in detrital zircon. Lithos 113, 570-582.

Bendall, B., Jensen-Schmidt, B., Holford, S., Dutch, R., Pawley, M., 2016. Insights into the nature and extent of sedimentary basins underlying the Eucla Basin from reprocessing and interpretation of the

13GA-EG1 Eucla-Gawler Seismic Survey, Australian Earth Sciences Convention, Adelaide, South Australia.

Blakey, R.C., 2008. Gondwana paleogeography from assembly to breakup - A 500 m.y. odyssey, In: Fielding, C.R., Frank, T.D., Isbell, J.L. (Eds.), Resolving the Late Paleozoic Ice Age in Time and Space. The Geological Society of America, Special Paper 441, Boulder, Colorado, pp. 1-28.

Blevin, J.E., Cathro, D.L., 2008. Australian Southern Margin Synthesis, Project GA707, pp. 1-104.

Blichert-Toft, J., Albarède, F., 1997. The Lu-Hf isotope geochemistry of chondrites and the evolution of the mantle-crust system. Earth and Planetary Science Letters 148, 243-258.

Bodorkos, S., Love, G.J., Nelson, D.R., Wingate, M.T.D., 2006. 149695: quartz sandstone, Quadrio Lake; Geochronology dataset 616, Compilation of geochronology data, June 2006 update. Western Australia Geological Survey.

Bradshaw, B.E., Rollet, N., Totterdell, J.M., Borissova, I., 2003. A revised structural framework for frontier basins on the Southern and Southwestern Australian Continental Margin. Geoscience Australia Record 2003/03, 1-94.

Brown, B.J., MüLler, R.D., Gaina, C., Struckmeyer, H.I.M., Stagg, H.M.J., Symonds, P.A., 2003. Formation and evolution of Australian passive margins: implications for locating the boundary between continental and oceanic crust, In: Hillis, R.R., Müller, R.D. (Eds.), Evolution and Dynamics of the Australian Plate. Geological Society of America.

Bryan, S.E., Cook, A.G., Allen, C.M., Siegel, C., Purdy, D.J., Greentree, J.S., Uysal, I.T., 2012. Early-mid cretaceous tectonic evolution of eastern Gondwana: From silicic LIP magmatism to continental rupture. Episodes 35, 142-152.

Carrapa, B., 2010. Resolving tectonic problems by dating detrital minerals. Geology 38, 191-192.

Cawood, P.A., Hawkesworth, C.J., Dhuime, B., 2012. Detrital zircon record and tectonic setting. Geology 40, 875-878.

Cawood, P.A., Korsch, R.J., 2008. Assembling Australia: Proterozoic building of a continent. Precambrian Research 166, 1-35.

Cawood, P.A., Nemchin, A.A., 2000. Provenance record of a rift basin: U/Pb ages of detrital zircons from the Perth Basin, Western Australia. Sedimentary Geology 134, 209-234.

Cawood, P.A., Nemchin, A.A., Freeman, M., Sircombe, K., 2003. Linking source and sedimentary basin: Detrital zircon record of sediment flux along a modern river system and implications for provenance studies. Earth and Planetary Science Letters 210, 259-268.

Clark, D.J., Hensen, B.J., Kinny, P.D., 2000. Geochronological constraints for a two-stage history of the Albany–Fraser Orogen, Western Australia. Precambrian Research 102, 155-183.

Clarke, G.L., Sun, S.-S., White, R.W., 1995. Grenville-age belts and associated older terranes in Australia and Antarctica. AGSO Journal of Australian Geology and Geophysics 16, 25-39.

Clarke, J.D.A., Gammon, P.R., Hou, B., Gallagher, S.J., 2003. Middle to Upper Eocene stratigraphic nomenclature and deposition in the Eucla Basin. Australian Journal of Earth Sciences 50, 231-248.

Cloetingh, S., Haq, B.U., 2015. Inherited landscapes and sea level change. Science 347.

Collins, A.S., 2003. Structure and age of the northern Leeuwin Complex, Western Australia: constraints from field mapping and U–Pb isotopic analysis. Australian Journal of Earth Sciences 50, 585-599.

Conrad, C.P., 2013. The solid Earth’s influence on sea level. Geological Society of America Bulletin 125, 1027-1052.

Czarnota, K., Hoggard, M.J., White, N., Winterbourne, J., 2013. Spatial and temporal patterns of Cenozoic dynamic topography around Australia. Geochemistry, Geophysics, Geosystems 14, 634-658.

Czarnota, K., Roberts, G.G., White, N.J., Fishwick, S., 2014. Spatial and temporal patterns of Australian dynamic topography from River Profile Modeling. Journal of Geophysical Research: Solid Earth 119, 1384-1424.

de Broekert, P., Sandiford, M., 2005. Buried Inset-Valleys in the Eastern Yilgarn Craton, Western Australia: Geomorphology, Age, and Allogenic Control. The Journal of Geology 113, 471-493.

de Gromard, R.Q., Wingate, M.T.D., Kirkland, C.L., Howard, H.M., Smithies, R.H., 2016. Geology and U-Pb geochronology of the Warlawurru Supersuite and MacDougall Formation in the Mitika and Wanarn areas, West Musgrave Province. Geological Survey of Western Australia, Record 2016/4, p. 29.

Dhuime, B.P.M., Hawkesworth, C., Storey, C.D., Cawood, P.A., 2011. From sediments to their source rocks. Geology 39, 407-410.

Dickinson, W.R., Suczek, C.A., 1979. Plate tectonics and sandstone compositions. AAPG Bulletin 63, 2164-2182.

Edgoose, C.J., 2013. Chapter 23: Amadeus Basin, In: Ahmad, M., Munson, T.J. (Eds.), Geology and mineral resources of the Northern Territory. Northern Territory Geological Survey, Special Publication 5.

Edgoose, C.J., Scrimgeour, I.R., Close, C.F., 2004. Geolog yof the Musgrave Block, Northern Territory. Northern Territory Geological Survey, Report 15, p. 46.

Evins, P.M., Kirkland, C.L., Wingate, M.T.D., Smithies, R.H., Howard, H.M., Bodorkos, S., 2012. Provenance of the 1340–1270 Ma Ramarama Basin in the west Musgrave Province, central Australia. Geological Survey of Western Australia, Report 116, p. 39.

Fielding, L., Najman, Y., Millar, I., Butterworth, P., Ando, S., Padoan, M., Barfod, D., Kneller, B., 2017. A detrital record of the Nile River and its catchment. Journal of the Geological Society 174, 301-317.

Fitzsimons, I.C.W., 2003. Proterozoic basement provinces of southern and southwestern Australia, and their correlation with Antarctica. Geological Society, London, Special Publications 206, 93-130.

Fraser, G.L., Neumann, N.L., 2016. Under the Nullarbor: New SHRIMP UPb zircon ages from the Coompana, Madura and Albany-Fraser Provinces, and Officer Basin, western South Australia and eastern Western Australia: July 2014-June 2015. Record 2016/16. Geoscience Australia, Canberra.

Gehrels, G.E., Valencia, V.A., Ruiz, J., 2008. Enhanced precision, accuracy, efficiency, and spatial resolution of U-Pb ages by laser ablation–multicollector–inductively coupled plasma–mass spectrometry. Geochemistry, Geophysics, Geosystems 9, n/a-n/a.

Goodge, J.W., Fanning, C.M., 2016. Mesoarchean and Paleoproterozoic history of the Nimrod Complex, central Transantarctic Mountains, Antarctica: Stratigraphic revisions and relation to the Mawson Continent in East Gondwana. Precambrian Research 285, 242-271.

Grey, K., Hocking, R.H., Stevens, M.K., Bagas, L., Carlsen, G.M., Irimies, F., Pirajno, F., Haines, P.W., Apak, S.N., 2005. Lithostratigraphic nomenclature of the Officer Basin and correlative parts of the Paterson Orogen, Western Australia. Western Australia Geological Survey, Report 93, p. 89.

Griffin, W.L., Belousova, E.A., Shee, S.R., Pearson, N.J., O’Reilly, S.Y., 2004. Archean crustal evolution in the northern Yilgarn Craton: U–Pb and Hf-isotope evidence from detrital zircons. Precambrian Research 131, 231-282.

Griffin, W.L., Pearson, N.J., Belousova, E., Jackson, S.E., van Achterbergh, E., O’Reilly, S.Y., Shee, S.R., 2000. The Hf isotope composition of cratonic mantle: LAM-MC-ICPMS analysis of zircon megacrysts in kimberlites. Geochimica et Cosmochimica Acta 64, 133-147.

Griffin, W.L., Pearson, N.J., Belousova, E.A., Saeed, A., 2007. Reply to “Comment to short-communication ‘Comment: Hf-isotope heterogeneity in zircon 91500' by W.L. Griffin, N.J. Pearson, E.A. Belousova and A. Saeed (Chemical Geology 233 (2006) 358–363)” by F. Corfu. Chemical Geology 244, 354-356.

Griffin, W.L., Wang, X., Jackson, S.E., Pearson, N.J., O'Reilly, S.Y., Xu, X., Zhou, X., 2002. Zircon chemistry and magma mixing, SE China: In-situ analysis of Hf isotopes, Tonglu and Pingtan igneous complexes. Lithos 61, 237-269.

Groves, D.I., Bierlein, F.P., 2007. Geodynamic settings of mineral deposit systems. Journal of the Geological Society 164, 19-30.

Groves, D.I., Santosh, M., 2015. Province-scale commonalities of some world-class gold deposits: Implications for mineral exploration. Geoscience Frontiers 6, 389-399.

Haines, P.W., Hocking, R.M., Grey, K., Stevens, M.K., 2008. Vines 1 revisited: are older Neoproterozoic glacial deposits preserved in Western Australia? Australian Journal of Earth Sciences 55, 397-406.

Haines, P.W., Kirkland, C.L., Wingate, M.T.D., Allen, H., Belousova, E.A., Gréau, Y., 2016. Tracking sediment dispersal during orogenesis: A zircon age and Hf isotope study from the western Amadeus Basin, Australia. Gondwana Research 37, 324-347.

Haines, P.W., Wingate, M.T.D., Kirkland, C.L., 2013. Detrital Zircon U–Pb ages from the Paleozoic of the Canning and Officer Basins, Western Australia: implications for provenance and interbasin connections. Proceedings of the West Australian Basins Symposium, sponsored by the Western Australian Branch of the Petroleum Exploration Society of Australia, Perth, 1-19.

Hawkesworth, C.J., Kemp, A.I.S., 2006. Using hafnium and oxygen isotopes in zircons to unravel the record of crustal evolution. Chemical Geology 226, 144-162.

Helby, R., Morgan, R., Partridge, A.D., 1987. A palynological zonation of the Australian Mesozoic, In: Jell, P.A. (Ed.), Studies in Australian Mesozoic Palynology. Memoir Association Australasian Palaeontologists, pp. 1-94.

Hocking, R.M., 1991. The Silurian Tumblagooda Sandstone, Western Australia. Geological Survey of Western Australia, Report 27.

Hou, B., Frakes, L.A., Sandiford, M., Worrall, L., Keeling, J., Alley, N.F., 2008. Cenozoic Eucla Basin and associated palaeovalleys, southern Australia — Climatic and tectonic influences on landscape evolution, sedimentation and heavy mineral accumulation. Sedimentary Geology 203, 112-130.

Hou, B., Keeling, J., Reid, A., Fairclough, M., Wairland, I., Belousova, E., Frakes, L., Hocking, R., 2011. Heavy mineral sands in the Eucla Basin, Southern Australia: depositional and province-scale prospectivity. Economic Geology 106, 687-712.

Huston, D.L., Blewett, R.S., Champion, D.C., 2012. Australia through time: a summary of its tectonic and metallogenic evolution. Episodes 35, 23-43.

Iizuka, T., Campbell, I.H., Allen, C.M., Gill, J.B., Maruyama, S., Makoka, F., 2013. Evolution of the African continental crust as recorded by U–Pb, Lu–Hf and O isotopes in detrital zircons from modern rivers. Geochimica et Cosmochimica Acta 107, 96-120.

Jackson, M.J., van de Graaff, W.J.E., 1981. Geology of the Officer Basin, Western Australia. Bureau of Mineral Resources, Geology and Geophysics, Bulletin 206.

Jackson, S.E., Pearson, N.J., Griffin, W.L., Belousova, E.A., 2004. The application of laser ablation-inductively coupled plasma-mass spectrometry to in situ U–Pb zircon geochronology. Chemical Geology 211, 47-69.

Jagodzinski, E.A., Dutch, R.A., 2013. SHRIMP Geochronology of the Tieyon (5645) 1:100000 mapsheet. Department for Manufacturing, Innovation, Trade, Resources and Energy, South Australia, Adelaide. Report Book 2013/00006, p. 222.

Jaques, A.L., Jaireth, S., Walshe, J.L., 2002. Mineral systems of Australia: an overview of resources, settings and processes. Australian Journal of Earth Sciences 49, 623-660.

JNOC, 1992. Geological and geophysical study in offshore Eucla Basins, Western Australia. Japan National Oil Corporation, Tokyo, Japan, p. 275.

Johnson, S.P., 2013. The birth of supercontinents and the Proterozoic assembly of Western Australia. Geological Survey of Western Australia.

Kemp, A.I.S., Hawkesworth, C.J., Paterson, B.A., Kinny, P.D., 2006. Episodic growth of the Gondwana supercontinent from hafnium and oxygen isotopes in zircon. Nature 439, 580-583.

Kirkland, C., xa, L, Stephen Daly, J., Whitehouse, M., xa, J, 2007. Provenance and Terrane Evolution of the Kalak Nappe Complex, Norwegian Caledonides: Implications for Neoproterozoic Paleogeography and Tectonics. The Journal of Geology 115, 21-41.

Kirkland, C.L., Smithies, R.H., Spaggiari, C.V., 2015a. Foreign contemporaries – Unravelling disparate isotopic signatures from Mesoproterozoic Central and Western Australia. Precambrian Research 265, 218-231.

Kirkland, C.L., Smithies, R.H., Spaggiari, C.V., Wingate, M.T.D., Quentin de Gromard, R., Clark, C., Gardiner, N.J., Belousova, E.A., 2017. Proterozoic crustal evolution of the Eucla basement, Australia: Implications for destruction of oceanic crust during emergence of Nuna. Lithos 278–281, 427-444.

Kirkland, C.L., Smithies, R.H., Woodhouse, A.J., Howard, H.M., Wingate, M.T.D., Belousova, E.A., Cliff, J.B., Murphy, R.C., Spaggiari, C.V., 2013a. Constraints and deception in the isotopic record; the crustal evolution of the west Musgrave Province, central Australia. Gondwana Research 23, 759-781.

Kirkland, C.L., Spaggiari, C.V., Smithies, R.H., Wingate, M.T.D., Belousova, E.A., Gréau, Y., Sweetapple, M.T., Watkins, R., Tessalina, S., Creaser, R., 2015b. The affinity of Archean crust on the Yilgarn—Albany–Fraser Orogen boundary: Implications for gold mineralisation in the Tropicana Zone. Precambrian Research 266, 260-281.

Kirkland, C.L., Wingate, M.T.D., Spaggiari, C.V., 2013b. 192557: metagabbro, Haig Cave, Perth, p. 4.

Kirkland, C.L., Wingate, M.T.D., Spaggiari, C.V., 2013c. 192558: granitic gneiss, Haig Cave, Perth, p. 4.

Korsch, R.J., Spaggiari, C.V., Occhipinti, S.A., Doublier, M.P., Clark, D.J., Dentith, M.C., Doyle, M.G., Kennett, B.L.N., Gessner, K., Neumann, N.L., Belousova, E., Tyler, I.M., Costelloe, R.D., Fomin, T., Holzschuh, J., 2014. Geodynamic implications of the 2012 Albany–Fraser deep seismic reflection survey: a transect from the Yilgarn Craton across the Albany–Fraser Orogen to the Madura Province, In: Spaggiari, C.V., Tyler, I.M. (Eds.), Albany–Fraser Orogen seismic and magnetotelluric (MT) workshop 2014 extended abstracts. Geological Survey of Western Australia, Record 2014/6, pp. 142-173.

Kositcin, N., 2010a. Geodynamic synthesis of the Gawler Craton and Curnamona Province. Geoscience Australia Record.

Kositcin, N., 2010b. Geodynamic Synthesis of the Gawler Craton and Curnamona Province. Geoscience Australia, Record, 2010/27.

Lancaster, P.J., Daly, J.S., Storey, C.D., Morton, A.C., 2017. Interrogating the provenance of large river systems: multi-proxy in situ analyses in the Millstone Grit, Yorkshire. Journal of the Geological Society 174, 75-87.

Leahy, K., Barnicoat, A.C., Foster, R.P., Lawrence, S.R., Napier, R.W., 2005. Geodynamic processes that control the global distribution of giant gold deposits. Geological Society, London, Special Publications 248, 119-132.

Lehmann, P.R., 1984. The stratigraphy, palaeogeography and petroleum potential of the Lower to lower Upper Devonian sequence in the Canning Basin. Petroleum Exploraiton Society of Australia, 253-275.

Lloyd, J., Collins, A.S., Payne, J.L., Glorie, S., Holford, S., Reid, A.J., 2016. Tracking the Cretaceous transcontinental Ceduna River through Australia: The hafnium isotope record of detrital zircons from offshore southern Australia. Geoscience Frontiers 7, 237-244.

Lowry, D.C., 1970. Geology of the Western Australian part of the Eucla Basin, In: Australia, G.S.o.W. (Ed.). Geological Survey of Western Australia, Perth, p. 207.

Ludwig, K.R., 2012. User's Manual for Isoplot/Ex, v.3.75, A Geochronological Toolkit for Microsoft Excel. Berkeley Geochronological Center Special Publications, 5.

MacDonald, J.D., Holford, S.P., Green, P.F., Duddy, I.R., King, R.C., Backé, G., 2013. Detrital zircon data reveal the origin of Australia's largest delta system. Journal of the Geological Society 170, 3-6.

Maidment, D.W., Williams, I.S., Hand, M., 2007. Testing long-term patterns of basin sedimentation by detrital zircon geochronology, Centralian Superbasin, Australia. Basin Research 19, 335-360.

Mark, C., Cogné, N., Chew, D., 2016. Tracking exhumation and drainage divide migration of the Western Alps: A test of the apatite U-Pb thermochronometer as a detrital provenance tool. Geological Society of America Bulletin.

McCann, T., Saintot, A., 2003. Tracing tectonic deformation using the sedimentary record: an overview. Geological Society, London, Special Publications 208, 1-28.

Morrissey, L.J., Payne, J.L., Hand, M., Clark, C., Taylor, R., Kirkland, C.L., Kylander-Clark, A., 2017. Linking the Windmill Islands, east Antarctica and the Albany–Fraser Orogen: Insights from U–Pb zircon geochronology and Hf isotopes. Precambrian Research 293, 131-149.

Müller, R.D., Flament, N., Matthews, K.J., Williams, S.E., Gurnis, M., 2016. Formation of Australian continental margin highlands driven by plate–mantle interaction. Earth and Planetary Science Letters 441, 60-70.

Nelson, D.R., 1997. Evolution of the Archaean granite-greenstone terranes of the Eastern Goldfields, Western Australia: SHRIMP U-Pb zircon constraints. Precambrian Research 83, 57-81.

Nelson, D.R., 1999. 154109: quartz-carbonate diamictite, Empress 1A, Compilation of geochronology data, 1998. Western Australia Geological Survey, Record 1999/2, pp. 190-193.

Nelson, D.R., 2002a. 154880: sandstone, Pirrilyungka Outstation; Geochronology dataset 259, Compilation of geochronology data, June 2006 update. Western Australia Geological Survey.

Nelson, D.R., 2002b. 154881: sandstone, Pirrilyungka Outstation; Geochronology dataset 260, Compilation of geochronology data, June 2006 update. Western Australia Geological Survey.

Nelson, D.R., 2004a. 154666: arenite, Empress 1A; Geochronology dataset 52, Compilation of geochronology data, June 2006 update. Western Australia Geological Survey.

Nelson, D.R., 2004b. 154667: sandstone, Empress 1A; Geochronology dataset 258, Compilation of geochronology data, June 2006 update. Western Australia Geological Survey.

Nelson, D.R., 2004c. 154668: sandstone, Empress 1A; Geochronology dataset 53, Compilation of geochronology data, June 2006 update. Western Australia Geological Survey.

Nelson, D.R., 2005a. 178070: amphibolite, Haig Cave; Geochronology dataset 596, Compilation of geochronology data, June 2006 update, Perth.

Nelson, D.R., 2005b. 178071: recrystallized biotite microtonalite, Haig Cave; Geochronology dataset 597, Compilation of geochronology data, June 2006 update, Perth.

Nelson, D.R., 2005c. 178072: tonalitic gneiss, Haig Cave; Geochronology dataset 598, Compilation of geochronology data, June 2006 update, Perth.

Neumann, N.L., Fraser, G.L., 2016. Under the Nullarbor: New SHRIMP U-Pb zircon ages from the Coompana, Madura and Albany-Fraser Provinces, and Officer Basin, western South Australia and eastern Western Australia. Commonwealth of Australia (Geoscience Australia).

Nichols, G., Jones, T.I.M., 1992. Fusain in Carboniferous shallow marine sediments, Donegal, Ireland: the sedimentological effects of wildfire. Sedimentology 39, 487-502.

O'Sullivan, G.J., Chew, D.M., Samson, S.D., 2016. Detecting magma-poor orogens in the detrital record. Geology 44, 871-874.

Partridge, A.D., 2006. Late Cretaceous palynology zonations for Australia, In: Monteil, E. (Ed.), Australian Mesozoic and Cenozoic palynology zonations - updated to the 2004 geologic timescale. Geoscience Australia, p. 8.

Paton, C., Hellstrom, J., Paul, B., Woodhead, J., Hergt, J., 2011. Iolite: Freeware for the visualisation and processing of mass spectrometric data. Journal of Analytical Atomic Spectrometry 26, 2508-2518.

Payne, J.L., Hand, M., Barovich, K.M., Reid, A., Evans, D.A.D., 2009. Correlations and reconstruction models for the 2500-1500 Ma evolution of the Mawson Continent. Geological Society, London, Special Publications 323, 319-355.

Pye, K., Tsoar, H., 2009. Aeolian sand and sand dunes. Springer-Verlag, Berlin.

Quigley, M.C., Clark, D., Sandiford, M., 2010. Tectonic geomorphology of Australia. Geological Society, London, Special Publications 346, 243-265.

Reid, A., Keeling, J., Boyd, D., Belousova, E., Hou, B., 2013. Source of zircon in world-class heavy mineral placer deposits of the Cenozoic Eucla Basin, southern Australia from LA-ICPMS U–Pb geochronology. Sedimentary Geology 286–287, 1-19.

Reid, A.J., Jagodzinski, E.A., Armit, R.J., Dutch, R.A., Kirkland, C.L., Betts, P.G., Schaefer, B.F., 2014. U-Pb and Hf isotopic evidence for Neoarchean and Paleoproterozoic basement in the buried northern Gawler Craton, South Australia. Precambrian Research 250, 127-142.

Reid, A.J., Korsch, R.J., Hou, B., Black, L.P., 2009. Sources of sediment in the Eocene Garford paleovalley, South Australia, from detrital-zircon geochronology. Australian Journal of Earth Sciences 56, S125-S137.

Requilme, L., 2016. Detrital Mineral Assemblage Analysis of Modern and Ancient Shorelines from Western Australia, Department of Applied Geology. Curtin University.

Reynolds, S., 2016. Stratigraphic evolution of the southern Australian onshore Bight Basin: a record for the breakup of Gondwana during the Cretaceous. Geological Survey of Western Australia Record 2016/11, p. 65.

Sandiford, M., 2007. The tilting continent: A new constraint on the dynamic topographic field from Australia. Earth and Planetary Science Letters 261, 152-163.

Scheib, A., Morris, P., Murdie, R., Delle Piane, C., 2016. A passive seismic approach to estimating the thickness of sedimentary cover on the Nullarbor Plain, Western Australia. Australian Journal of Earth Sciences 63, 583-598.

Schellart, W.P., Spakman, W., 2015. Australian plate motion and topography linked to fossil New Guinea slab below Lake Eyre. Earth and Planetary Science Letters 421, 107-116.

Scherer, E., Münker, C., Mezger, K., 2001. Calibration of the Lutetium-Hafnium Clock. Science 293, 683-687.

Shaanan, U., Rosenbaum, G., Sihombing, F.M.H., 2017. Continuation of the Ross–Delamerian Orogen: insights from eastern Australian detrital-zircon data. Australian Journal of Earth Sciences, 1-9.

Sircombe, K.N., Freeman, M.J., 1999. Provenance of detrital zircons on the Western Australia coastline—Implications for the geologic history of the Perth basin and denudation of the Yilgarn craton. Geology 27, 879-882.

Sláma, J., Košler, J., Condon, D.J., Crowley, J.L., Gerdes, A., Hanchar, J.M., Horstwood, M.S.A., Morris, G.A., Nasdala, L., Norberg, N., Schaltegger, U., Schoene, B., Tubrett, M.N., Whitehouse, M.J., 2008. Plešovice zircon — A new natural reference material for U–Pb and Hf isotopic microanalysis. Chemical Geology 249, 1-35.

Spaggiari, C.V., Kirkland, C.L., Smithies, R.H., Wingate, M.T.D., 2014. Tectonic links between Proterozoic sedimentary cycles, basin formation and magmatism in the Albany–Fraser Orogen. Geological Survey of Western Australia, Report 133, p. 63.

Spaggiari, C.V., Kirkland, C.L., Smithies, R.H., Wingate, M.T.D., Belousova, E.A., 2015. Transformation of an Archean craton margin during Proterozoic basin formation and magmatism: The Albany–Fraser Orogen, Western Australia. Precambrian Research 266, 440-466.

Spaggiari, C.V., Smithies, R.H., 2015. Eucla basement stratigraphic drilling results release workshop: extended abstracts, p. 70.

Spencer, C.J., Kirkland, C.L., Taylor, R.J.M., 2016. Strategies towards statistically robust interpretations of in situ U–Pb zircon geochronology. Geoscience Frontiers 7, 581-589.

Totterdell, J.M., Blevin, J.E., Struckmeyer, H.I.M., Bradshaw, B.E., Colwell, J.B., Kennard, J.M., 2000. A New Sequence Framework for the Great Australian Bight: Starting with a Clean Slate. Australian Petroleum Production & Exploration Association 40, 95-117.

Totterdell, J.M., Bradshaw, B.E., 2004. The structural framework and tectonic evolution of the Bight Basin, In: Boult, P.J., Johns, D.R., Lang, S.C. (Eds.), Eastern Australasian Basins Symposium II. Petroleum Exploration Society of Australia, Special Publication, pp. 41-61.

Totterdell, J.M., Krassay, A.A., 2003. Sequence stratigraphic correlation of onshore and offshore Bight Basin successions. Geoscience Australia Record 2003/02, p. 50.

Tucker, R.T., Roberts, E.M., Henderson, R.A., Kemp, A.I.S., 2016. Large igneous province or long-lived magmatic arc along the eastern margin of Australia during the Cretaceous? Insights from the sedimentary record. Geological Society of America Bulletin 128, 1461-1480.

Tyrrell, S., Haughton, P.D.W., Daly, J.S., 2007. Drainage reorganization during breakup of Pangea revealed by in-situ Pb isotopic analysis of detrital K-feldspar. Geology 35, 971-974.

Veevers, J.J., Belousova, E.A., Saeed, A., 2016. Zircons traced from the 700–500 Ma Transgondwanan Supermountains and the Gamburtsev Subglacial Mountains to the Ordovician Lachlan Orogen, Cretaceous Ceduna Delta, and modern Channel Country, central-southern Australia. Sedimentary Geology 334, 115-141.

Veevers, J.J., Belousova, E.A., Saeed, A., Sircombe, K., Cooper, A.F., Read, S.E., 2006. Pan-Gondwanaland detrital zircons from Australia analysed for Hf-isotopes and trace elements reflect an ice-covered Antarctic provenance of 700–500 Ma age, TDM of 2.0–1.0 Ga, and alkaline affinity. Earth-Science Reviews 76, 135-174.

Veevers, J.J., Saeed, A., Belousova, E.A., Griffin, W.L., 2005. U–Pb ages and source composition by Hf-isotope and trace-element analysis of detrital zircons in Permian sandstone and modern sand from southwestern Australia and a review of the paleogeographical and denudational history of the Yilgarn Craton. Earth-Science Reviews 68, 245-279.

Vermeesch, P., 2013. Multi-sample comparison of detrital age distributions. Chemical Geology 341, 140-146.

Vermeesch, P., Resentini, A., Garzanti, E., 2016. An R package for statistical provenance analysis. Sedimentary Geology 336, 14-25.

Wiedenbeck, M., AllÉ, P., Corfu, F., Griffin, W.L., Meier, M., Oberli, F., Quadt, A.V., Roddick, J.C., Spiegel, W., 1995. Three natural zircon standards for U-Th-Pb, Lu-Hf, trace element and REE analyses. Geostandards Newsletter 19, 1-23.

Willcox, J.B., Stagg, H.M.J., 1990. Australia's southern margin: a product of oblique extension. Tectonophysics 173, 269-281.

Wingate, M.T.D., Bodorkos, S., 2007a. 181126: quartz sandstone, Durba Spring; Geochronology dataset 681, Compilation of geochronology data. Western Australia Geological Survey.

Wingate, M.T.D., Bodorkos, S., 2007b. 181871: quartz sandstone, Lancer 1; Geochronology dataset 683, Compilation of geochronology data. Western Australia Geological Survey.

Wingate, M.T.D., Bodorkos, S., 2007c. 181872: quartz sandstone, Lancer 1; Geochronology dataset 684, Compilation of geochronology data. Western Australia Geological Survey.

Wingate, M.T.D., Bodorkos, S., 2007d. 181873: quartz sandstone, Lancer 1; Geochronology dataset 685, Compilation of geochronology data. Western Australia Geological Survey.

Wingate, M.T.D., Kirkland, C.L., Haines, P.W., Hocking, R.M., 2013. 199424: sandstone, Empress 1; Geochronology Record 1113. Geological Survey of Western Australia.

Wingate, M.T.D., Kirkland, C.L., Spaggiari, C.V., Smithies, R.H., 2015. U-Pb geochronology of the Madura Province, In: Spaggiari, C.V., Smithies, R.H. (Eds.), Eucla basement stratigraphic drilling results release workshop: extended abstracts. Geological Survey of Western Australia, Record 2015/10, pp. 14-16.

Wingate, M.T.D., Lu, Y., Spaggiari, C.V., Smithies, R.H., 2016. 206754: metagranodiorite, Madura Province, Perth, p. 4.

Wyborn, L.A.I., Heinrich, C.A., Jaques, A.L., 1994. Australian Proterozoic mineral systems: essential ingredients and mappable criteria. Australasian Institute of Mining and Metallurgy Publications Series 5/94, 109-115.

Xu, J., Snedden, J.W., Stockli, D.F., Fulthorpe, C.S., Galloway, W.E., 2016. Early Miocene continental-scale sediment supply to the Gulf of Mexico Basin based on detrital zircon analysis. Geological Society of America Bulletin.